A Set Theoretic Approach to Dynamic Robot Localization and Mapping

M. Di Marco, A. Garulli, A. Giannitrapani, A. Vicino *

Abstract

This paper addresses the localization and mapping problem for a robot moving through a (possibly) unknown environment where indistinguishable landmarks can be detected. A set theoretic approach to the problem is presented. Computationally efficient algorithms for measurement-to-feature matching, estimation of landmark positions, estimation of robot location and heading are derived, in terms of uncertainty regions, under the hypothesis that errors affecting all sensors measurements are unknown-but-bounded. The proposed technique is validated in both simulation and experimental setups.

Keywords: Localization, Mapping, SLAM, Uncertainty, Set Membership.

1   Introduction

Recent years have witnessed a growing interest towards mobile robots and their use in hostile and unknown environments: several industrial and scientific research projects are aimed at obtaining increased autonomy of mobile robots, in order to be independent of the intervention of human operators. To operate successfully, the robot must be able to localize itself in the environment (Leonard and Durrant-Whyte 1991, Shastri 1999). In fact, it is well recognized that robot self localization is one of the most important problems for long range autonomous navigation. Several techniques have been proposed in order to allow the robot to precisely determine its own position and orientation (the robot *pose*). Those techniques depend on the robot sensory systems, the environment the vehicle is navigating in, and the a priori knowledge available to the robot.

There are basically two different approaches to localization (see e.g. (Fox, Burgard and Thrun 1999)). *Tracking* or *local* techniques aim at developing algorithms that incrementally update the robot position, while *global* techniques are designed to estimate the robot pose even under global uncertainty, i.e. without any a priori information on the robot location. Since information provided

---
*The authors are with the Dipartimento di Ingegneria dell'Informazione, Università di Siena, Via Roma, 56 — 53100 Siena, Italy. Email: {dimarco, garulli, giannitrapani, vicino}@dii.unisi.it

by proprioceptive sensors (e.g., dead-reckoning) is prone to systematic errors and error accumulation (Cox 1991, Barshan and Durrant-Whyte 1995), most recent works dealing with local techniques suggest to combine dead-reckoning with some additional localization methods, generally based on measurements performed on the environment. Fusion of the two kinds of information is usually obtained via filtering techniques, the Extended Kalman Filter (EKF) being the most popular (see, e.g., (Leonard and Durrant-Whyte 1991, Cox 1991, Holenstein and Badreddin 1992)). In the above cases, robot position uncertainty is modeled as a unimodal Gaussian distribution, and white Gaussian zero-mean random processes are generally used to represent unmodeled robot dynamics and sensor noises. However, in many cases, real-world disturbances do not satisfy the above statistical assumptions. Therefore, different techniques have been investigated: in (Kieffler, Jaulin, Walter and Meizel 1999, Garulli and Vicino 2001, Victorino, Rives and Borrelly 2002) Set Membership estimation techniques are applied to the case of distinguishable landmarks, while in (Hanebeck and Horn 1999) a mixed statistical/set-theoretic approach to the estimation problem is proposed.

In the development of global techniques, several different methods have been proposed: search for matching between map and measurements (Drumheller 1987, Talluri and Aggarwal 1992), identification of landmarks and triangulation (Mouaddib and Marhic 2000, Levitt and Lawton 1990, Sutherland and Thompson 1994, Betke and Gurvits 1997), use of occupancy grids (Elfes 1987) and Markov techniques (Fox, Burgard and Thrun 1998), minimization of Hausdorff distance between local and global map (Olson 2000), multiple hypothesis tracking combining Kalman filtering and Markov estimation (Jensfelt and Kristensen 1999, Roumeliotis and Bekey 2000, Reuter 2000).

More recently, driven by the interest in planetary exploration, researches have turned their attention towards localization of vehicles moving in unknown hostile environments (Olson 2000, Lacroix, Mallet, Chatila and Gallo 1999). In this case, a map of the environment is not available, and hence the more complex Simultaneous Localization and Map building (SLAM) problem must be tackled. The robot has to collect information about the environment, and at the same time it must localize itself in the map it is building. The most common approach to the problem is based on Kalman filtering (Moutarlier and Chatila 1989, Leonard and Durrant-Whyte 1992, Gibbens, Dissanayake and Durrant-Whyte 2000): it provides a recursive solution to the navigation problem and a technique for computing estimates of uncertainty for both the vehicle and the landmarks. Unfortunately, in order to guarantee consistency of the filtered quantities, all the correlations among landmarks must be estimated (Uhlmann, Julier and Csorba 1997, Castellanos and Tardos 1999), thus requiring high computational resources. In addition, to obtain a quantitative evaluation of the estimation errors, suitable assumptions on the distribution of sensor noises must be introduced. This kind of assumptions on landmark perception and robot motion are seldom satisfied on natural terrains, since the complexity of the process of extracting low level data makes it difficult to obtain a complete error analysis (Sabater and Thomas 1991). Consequently, other techniques, different from the Kalman filter, have been investigated. These approaches include Markov localization and Bayes rule (Thrun, Burgard and Fox 1998), occupancy grids (Elfes 1991) and iconic matching (Olson 2000). Another possible approach to the SLAM problem is based on topological maps

(Levitt and Lawton 1990, Brooks 1986, Mataric 1992). Instead of building a metrically accurate description, this method employs a qualitative knowledge of the relative position of landmarks and robot to build maps and guide motion. Efforts have been spent to merge together topological and feature-based approaches (Kurz 1996).

In this paper we will address the localization problem for a robot, equipped with proprioceptive sensors (e.g., odometers and compass), moving through a (possibly) unknown environment. We assume that the robot is equipped with suitable exteroceptive sensors which permit to detect indistinguishable landmarks in the environment and to get relative measurements of its position and heading with respect to landmarks. In addition, we suppose that the robot is moving in a basically flat environment, such that a 2D dynamic model can be adopted. Different from what is done in most of the literature, no statistical assumption is made on the errors affecting the sensors; the only assumption is that they are bounded in norm by some quantity. This leads quite naturally to a set theoretic approach to the problem. Estimates of the unknown quantities are derived in terms of *feasible uncertainty sets*, defined as the regions where those quantities are guaranteed to lie, according to the available information. Those sets provide a quantitative description of the estimation errors. It is shown that set membership uncertainty representation can be exploited to obtain a correct matching between measurements and detected landmarks. Moreover, the same approach is adopted to tackle the SLAM problem, by including landmark positions in the state vector to be estimated.

The basic reference theory for the technical development of the paper relies in the recently developed set membership estimation theory (see, e.g, (Milanese and Vicino 1991, Kurzhanski and Veliov 1994, Milanese, Norton, Piet-Lahanier and Walter 1996)). Though most of the theory is developed for linear estimation, we will exploit the specific structure of the nonlinear localization problem to get efficient solutions, based on recursive approximations of the uncertainty regions. One of the first papers in which the set theoretic paradigm has been applied to robotic localization is (Sabater and Thomas 1991), in which fusion of multiple sensor information with bounded uncertainty is used to construct a geometric representation of features in the environment. Set membership localization based on angle measurements has been tackled in (Hanebeck and Schmidt 1996, Garulli and Vicino 2001), using different set approximation techniques. A set-based localization algorithm using images from a stereo vision system has been proposed in (Atiya and Hager 1993). Preliminary ideas on how to deal with the SLAM problem in the presence of bounded errors are given in (Di Marco, Garulli, Lacroix and Vicino 2000).

The aim of the present paper is to provide a general set-theoretic framework, in which the classical problems involved with autonomous robot navigation, such as localization and simultaneous localization and map building, can be tackled. Computationally efficient set membership algorithms for dynamic localization and mapping are constructed, exploiting state decomposition and set approximations.

The paper is organized as follows. Section 2 illustrates how set-valued methods can be employed to solve the localization problems. More specifically, algorithms performing localization in known envi-

ronments, measurement-to-feature matching, and localization in (partially or completely) unknown environments are presented. Section 3 concerns the implementation of such algorithms: the high computational burden of the algorithms presented in Section 2 can be reduced via state decomposition and set approximation. Section 4 reports numerical simulations and experimental results, while some conclusions are drawn in Section 5.

2 Set-Valued Methods for Localization

2.1 Models, assumptions and problem formulation

Let us consider a vehicle navigating in a 2D environment, and let

$$p(k) = [x(k) \ y(k) \ \theta(k)]' \in \mathcal{Q} \triangleq \mathbb{R}^2 \times [-\pi \ \pi]$$

be the pose of the agent at time k, where $(x(k), y(k))$ denotes the robot position, and $\theta(k)$ represents the robot heading w.r.t. the positive x-axis. Time evolution of the robot pose $p(k)$ can be described by a suitable dynamic model. Under the assumption of slow robot dynamics, if translation and rotation measurements $u(k)$ from odometric sensors are available, the vehicle dynamics can be described by the linear discrete-time model

$$p(k + 1) = p(k) + u(k) + w(k), \tag{1}$$

where $w(k) \in \mathbb{R}^3$ models the error affecting measurements $u(k)$. Nonetheless, the technique presented in this paper applies to the general linear time-varying model

$$\eta(k + 1) = F(k)\eta(k) + G(k)u(k) + H(k)w(k), \tag{2}$$

where $\eta(k) \triangleq [p'(k) \ \dot{p}'(k)]'$ represents the robot state vector. Notice that model (2) can be adopted to approximate any nonlinear dynamics $\dot{\eta}(t) = f(\eta(t), u(t), w(t))$ through discretization and linearization w.r.t. the current robot state.

The robot is equipped with exteroceptive sensors, providing measurements on the environment. In this paper, it is assumed that the environment can be described by landmarks, i.e. indistinguishable features represented by points on a plane. When navigating in a 2D environment, a sensing robot has usually access to two kinds of measurements: (i) distance from a landmark; (ii) angle between robot orientation and the direction of a landmark. The former is usually provided by sensors such as ultrasonic or infrared sensors, the latter is given by panoramic cameras. Alternative sensors (such as millimeter-wave radars, laser rangefinders and stereovision systems) provide both kinds of information. All these measurements can be modeled as nonlinear functions of the robot pose $p(k)$ and the position of the landmark $l_i = [x_{l_i} \ y_{l_i}]'$ with respect to which the measurement is taken. In the first part of this section, it is assumed that landmarks l_i, $i = 1, \ldots, n$, have been correctly recognized and their position is known exactly (i.e. an accurate environment map is given a priori). This assumption will be relaxed in Sections 2.3-2.4. In order to fix the main ideas behind

the proposed approach, it is assumed that both distance and angle measurements are available to the robot (see Figure 1); thus, measurement equations take on the form

$$
\begin{aligned}
D_i(k) &= d(p(k), l_i) + v_{d_i}(k) \\
A_i(k) &= \alpha(p(k), l_i) + v_{\alpha_i}(k)
\end{aligned}
\qquad i = 1, \ldots, m,
\tag{3}
$$

where m is the number of measurements performed at time k, $D_i(k)$ and $A_i(k)$ are the actual readings provided by the sensors at time k; $v_{d_i}(k)$ and $v_{\alpha_i}(k)$ are measurement noises affecting the distance and the heading measurements respectively, defined as

$$
\begin{aligned}
d(p(k), l_i) &\triangleq \sqrt{(x(k) - x_{l_i})^2 + (y(k) - y_{l_i})^2} \\
\alpha(p(k), l_i) &\triangleq \mathrm{atan}_2(y_{l_i} - y(k), x_{l_i} - x(k)) - \theta(k),
\end{aligned}
\tag{4}
$$

with $\mathrm{atan}_2(b, a)$ denoting the four quadrant inverse tangent. Notice that function $d(\cdot)$ depends on the robot position only, while function $\alpha(\cdot)$ is related to both position and heading.
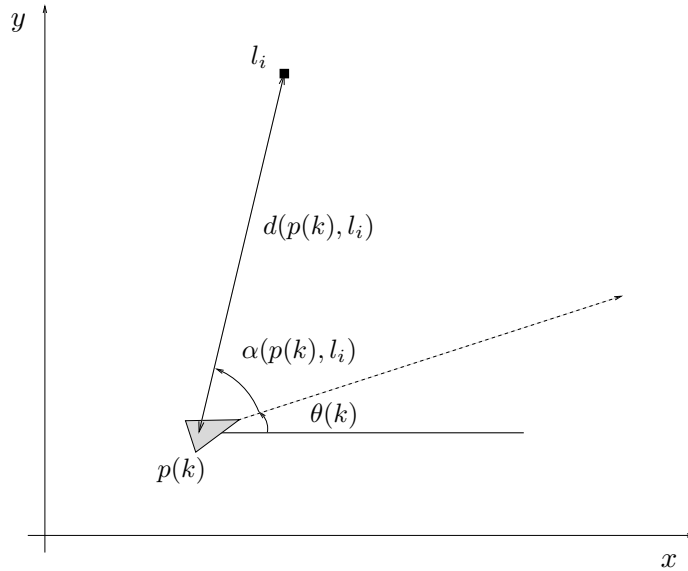

PSfrag replacements

Figure 1: Distance and relative orientation measurements with respect to an identified landmark.

The dynamic localization problem can be stated as follows.

Dynamic Localization Problem: Let $\hat{p}(0)$ be an estimate of the initial robot pose. Given the dynamic model (1) and the measurement equations (3)-(4), compute an estimate $\hat{p}(k)$ of the vehicle pose $p(k)$ at each time instant $k = 1, 2, \ldots$.

This problem can be tackled in different ways, depending on the hypotheses on the unknown disturbances $w(k)$, $v_{d_i}(k)$ and $v_{\alpha_i}(k)$ in (1) and (3). When statistical assumptions on the errors are considered, the estimate of the pose can be computed via the extended Kalman filter (Leonard and Durrant-Whyte 1991), or using Markov localization and Bayes rules (Fox et al. 1998). However, real-world uncertainties may include also systematic errors or nongaussian, colored noise, whose

statistical properties are generally very difficult to estimate. In this paper, a different approach is presented, based on the assumption that the disturbances are unknown-but-bounded (UBB), i.e.

$$\|w(k)\|_\infty \leq \epsilon^w \tag{5}$$

$$|v_{d_i}(k)| \leq \epsilon^{v_d} \tag{6}$$

$$|v_{\alpha_i}(k)| \leq \epsilon^{v_\alpha} \tag{7}$$

where ϵ^w, ϵ^{v_d} and ϵ^{v_α} are known positive scalars, and $\|\cdot\|_\infty$ denotes the $\infty-$norm (defined as $\|v\|_\infty = \max_i |v_i|$). We observe that the above bounds need not be constant for different time instants k, or for different components of vector $w(k)$ (which is equivalent to consider a weighted ℓ_∞ norm). For simplicity of notation, this feature will not be considered in the treatment of the paper, the extension being straightforward.

Assumptions (6) and (7) allow one to define the notion of feasible state vector. Given sensor readings $D_i(k)$, $A_i(k)$, $i = 1, \ldots, m$, the feasible states are those compatible with all the measurements, i.e. the states belonging to the *measurement set*

$$\mathcal{M}(k) = \bigcap_{i=1}^m \mathcal{M}_i(k). \tag{8}$$

where

$$\mathcal{M}_i(k) = \{p : \ |D_i(k) - d(p(k), l_i)| \leq \epsilon^{v_d} \text{ and } |A_i(k) - \alpha(p(k), l_i)| \leq \epsilon^{v_\alpha}\}. \tag{9}$$

Notice that, if assumptions (6) and (7) are verified, the set $\mathcal{M}$ is not empty. On the other hand, an empty intersection implies that at least one of the constraints (6) and (7) is violated. A direct consequence is that the dynamic localization problem can be formulated in a set-theoretic framework.

SM localization problem: Let $P(0) \subset \mathcal{Q}$ be a set containing the initial pose $p(0)$. Given the dynamical model (1) and the measurement equations (3)-(4), find at each time $k = 1, 2, \ldots$, the *feasible pose set $P(k|k) \subset \mathcal{Q}$* containing all vehicle poses $p(k)$ that are compatible with the robot dynamics, the assumptions (5)-(7) on the disturbances and the measurements collected up to time k.

The shape of each set $\mathcal{M}_i(k)$ depends on the nonlinear functions modeling each measurement process. It is easily verified that for any distance measurement $D_i(k)$, the corresponding measurement set is a portion of $\mathcal{Q}$ whose shape is a cylindrical circular corona, see Figure 2a. On the other hand, relative orientation measurements provide sets that are portions of $\mathcal{Q}$ delimited by two helicoids (a part of this set, limited in the (x, y) plane, is shown in Figure 2b). The intersection of the two sets depicted in Figure 2, which corresponds to (9), is given by the roto-translation of a sector of corona, around and along the i-th landmark position axis. The shape of such a set is reported in Figure 3.
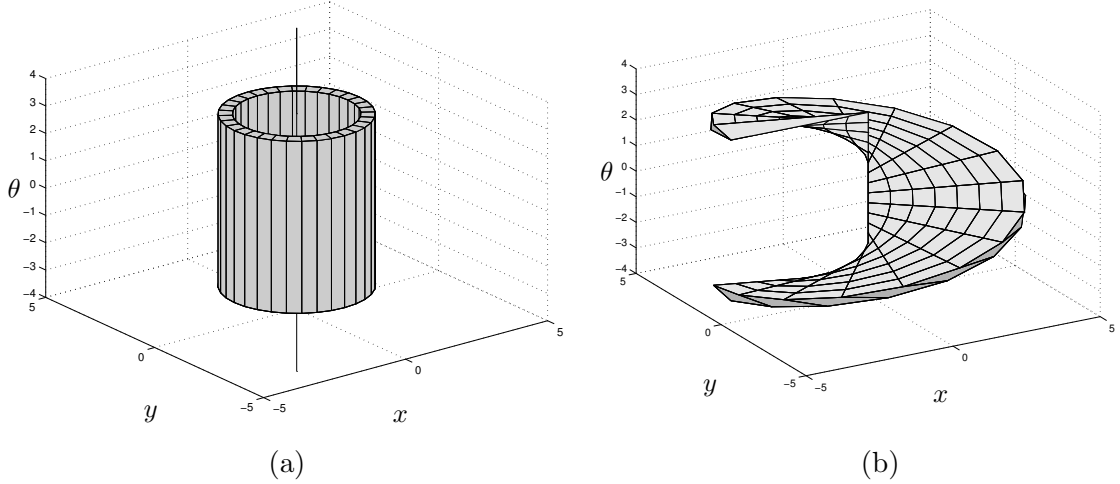
(a)
(b)

Figure 2: Measurement sets associated to distance (a) and relative orientation measurements (b).

2.2 Solution to SM localization problem

The solution to the SM localization problem is given by the following recursion, which stems out directly from (1) and (3)-(4)

$$P(0|0) = P(0), \tag{10}$$

$$P(k+1|k) = P(k|k) + u(k) + \text{Diag}[\epsilon^w]\mathcal{B}_\infty, \tag{11}$$

$$P(k+1|k+1) = P(k+1|k) \cap \mathcal{M}(k+1), \tag{12}$$

where $\mathcal{B}_\infty$ is the unit ball in the $\infty-$norm and $\text{Diag}[v]$ denotes the diagonal matrix with vector v on the diagonal. Algebraic operators in (11) and (12) are to be intended as set operators. Equation (11) is often referred to as time update: during this step, information provided by the robot dynamic model and odometric sensors are used to update the feasible set. The set $\text{Diag}[\epsilon^w]\mathcal{B}_\infty$ describes all the admissible unmodeled dynamics and odometric errors satisfying assumption (5); due to these disturbances, the size of the feasible pose set grows during the time update. Equation (12) is known as measurement update as it exploits all the exteroceptive measurements to reduce the total robot uncertainty. The main property of recursion (10)-(12) is to provide, at each time step, all the pose values that are compatible with the available information: the true state is guaranteed to belong to set $P(k|k)$, and the size of such set gives a measure of the uncertainty associated to the estimate. Unfortunately, the exact computation of sets $P(k|k)$ is generally very difficult, because the measurement set $\mathcal{M}(k)$ is the intersection of nonconvex sets. Nonetheless, the problem can be tackled by applying set approximation techniques, as it will be shown in Section 3.

2.3 Matching

The localization algorithm provided by equations (10)-(12) assumes that the robot is able to correctly associate each measurement to the corresponding measured feature. For example, this hap-
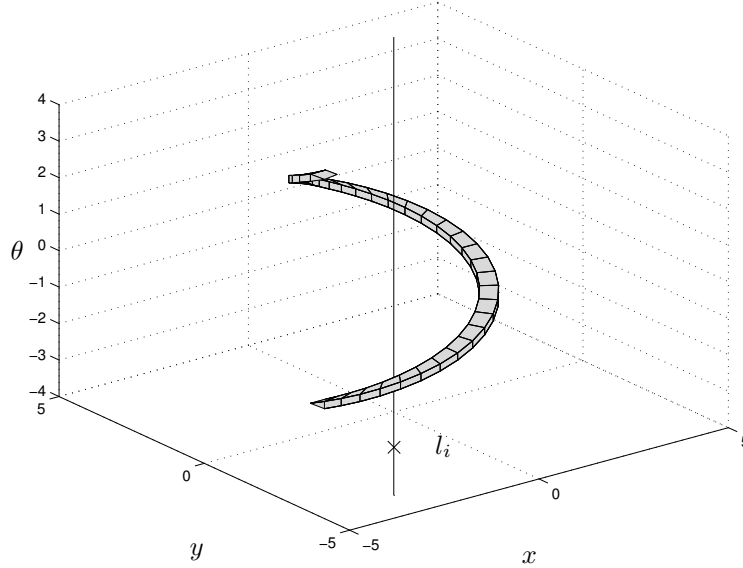
Figure 3: Measurement set $\mathcal{M}_i$ associated to the pair of measurements (3).

pens if the observed landmarks are distinguishable. However, in real-world applications, especially if natural beacons are used as landmarks and sensors provide only metric information, landmarks are indistinguishable and consequently matching between measurements and landmarks is of paramount importance. Within the set-theoretic framework, it is possible to exploit the properties of the feasible sets to evaluate all the admissible matchings, i.e. all the associations measurement-landmark that are compatible with the assumptions.

In the following, subscripts xy and θ represent the projection of a set (or a vector) on the robot position and orientation subspaces, respectively.

At time k, the predicted robot uncertainty set, before measurements are taken, is given by $P(k|k-1)$. Thus, $P_{xy}(k|k-1)$ is the predicted position uncertainty set, and $P_\theta(k|k-1)$ the predicted orientation uncertainty interval. A measurement pair D_i, A_i guarantees that, in a robot centered 2D reference system, landmark l_i lies in the set

$$\mathcal{M}_{l_i}(k) = \left\{ l \in \mathbb{R}^2 : \ |D_i(k) - d(0, l)| \leq \epsilon^{v_d} \text{ and } |A_i(k) - \alpha(0, l) + \hat{\theta}| \leq \epsilon^{v_\alpha} + \epsilon^{\hat{\theta}} \right\} \tag{13}$$

where $[\hat{\theta} - \epsilon^{\hat{\theta}}, \ \hat{\theta} + \epsilon^{\hat{\theta}}] = P_\theta(k|k-1)$. Notice that the actual robot orientation uncertainty $P_\theta(k|k-1)$ has been exploited in (13). Hence, the set in which the $i-th$ landmark is guaranteed to lie on the basis of the robot uncertainty and measurements taken at time k is $P_{xy}(k|k-1) + \mathcal{M}_{l_i}(k)$. As a consequence, any landmark position $l_j, j = 1, \ \ldots, n$ such that $l_j \in P_{xy}(k|k-1) + \mathcal{M}_{l_i}(k)$, can be associated to the i-th measurement (see Figure 4).

By repeating the process for each measurement pair, it is possible to build a matching matrix T, where all the admissible matchings measurement-landmark are listed. To do this, one can set $t_{ij} = 1$ if the j-th landmark lies inside $P_{xy}(k|k-1) + \mathcal{M}_{l_i}(k)$, while $t_{ij} = 0$ otherwise. If on the i-th row of matrix T there is only one non zero entry, then the i-th measurement is not ambiguous. Should
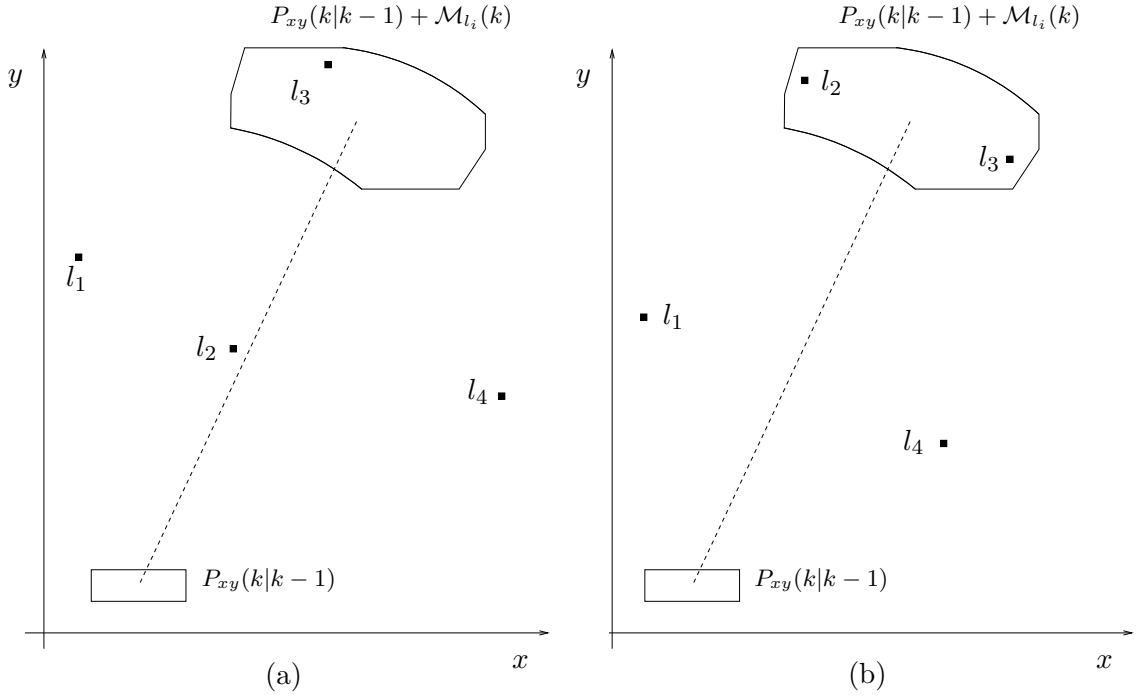
Figure 4: Uncertainty sets can be employed to perform matching between measurements and features. (a) Measurement i is not ambiguous, since only landmark l_3 lies in $P_{xy}(k|k-1) + \mathcal{M}_{l_i}(k)$; (b) Measurement i is ambiguous, since it can be associated both to landmark l_2 and to landmark l_3.

all the entries be null, than there is no landmark compatible with the measurement (consequently, the i-th measurement is an outlier). Finally, a row with more than one nonzero entry, indicates an ambiguous measurement (see Figure 5).

Even if some measurement is ambiguous, it is often possible to find a unique admissible solution to the matching problem (see Figure 6). Indeed, the problem of determining the existence of a perfect matching is widely studied in the operation research field, and efficient algorithms are available to determine the solution of such problems (Korte and Vygen 2000). Uniqueness of the perfect matching can be tested by removing from the associated graph, one at a time, each solution branch, and verifying that no other solution is available.

In principle, even if the solution to the matching problem is not unique, the algorithm described in (10)-(12) is still appropriate to solve the localization problem: as a matter of fact, for any possible perfect matching μ, $\mu = 1, \ldots, p$, one has to evaluate the corresponding measurement set $\mathcal{M}^\mu(k) = \cap_{i=1}^m \mathcal{M}_i^\mu(k)$ in (8). To account for all possible distinct choices in the matching step, one has to replace equation (12) with

$$P(k+1|k+1) = P(k+1|k) \cap \left[\cup_{\mu=1}^p \mathcal{M}^\mu(k+1)\right], \tag{14}$$

where set $\cup_{\mu=1}^p \mathcal{M}^\mu$ replaces the single measurement set available when landmark identification is a priori known. Notice that, when performing the matching step, robot uncertainty $P(k|k-1)$

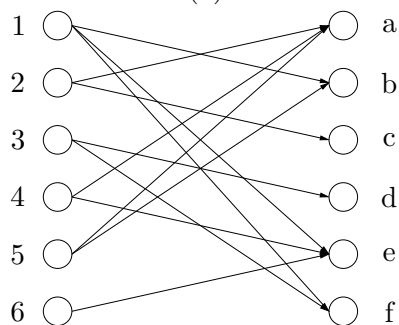| meas.\land.	a	b	c	d	e	f
1	0	1	0	0	1	1
2	1	0	1	0	0	0
3	0	0	0	1	0	1
4	0	0	0	0	0	0
5	1	0	0	0	0	0
6	0	0	0	0	1	0

(a)
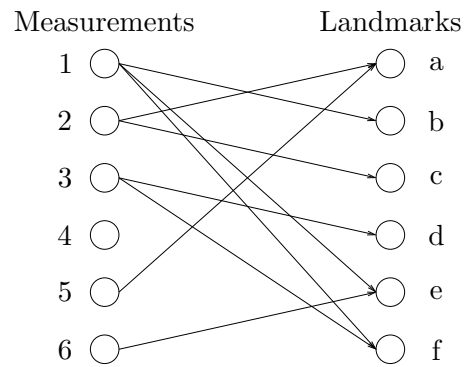
(b)

Figure 5: (a) Example of matching matrix T: according to the matrix, the first 3 measurements are ambiguous, the fourth is spurious, while the last 2 are compatible with only one landmark: (b) The corresponding graph.

meas.\land.	a	b	c	d	e	f
1	0	1	0	0	1	1
2	1	0	1	0	0	0
3	0	0	0	1	0	1
4	1	0	0	0	1	0
5	1	1	0	0	0	0
6	0	0	0	0	1	0

(a)

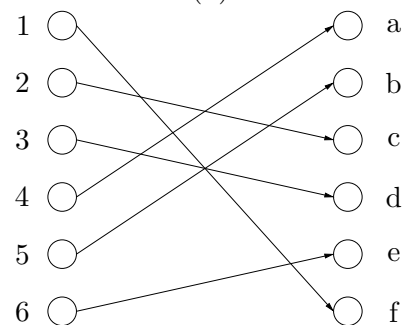| meas.\land.	a	b	c	d	e	f
1	0	0	0	0	0	1
2	0	0	1	0	0	0
3	0	0	0	1	0	0
4	1	0	0	0	0	0
5	0	1	0	0	0	0
6	0	0	0	0	1	0

(b)

Figure 6: The ambiguity of some measurements in matrix T is compatible with the existence and uniqueness of a perfect matching: (a) matrix T with ambiguous measurements; (b) unique admissible matching.

needs to be considered in order to correctly determine all the admissible perfect matchings. Once the aforementioned matchings are available, the evaluation of each measurement set $\mathcal{M}^\mu$ does not depend on the robot position uncertainty. Consequently, some of the sets $\mathcal{M}^\mu$ may turn out to be empty, thus allowing to deem a posteriori that matching μ is not correct.

2.4   Uncertain landmarks

In this section, we will consider the case when the position of the landmarks is not exactly known. This situation occurs in two different problems: (i) localization with uncertain maps, in which it is known that landmarks lie in given sets; (ii) exploration and mapping of unknown environments, where the position of the landmarks is unknown and must be estimated together with the robot pose. The latter is a well-known hard challenge in mobile robotics, usually addressed as Simultaneous Localization And Map building (SLAM) problem. The two problems can be tackled within the same framework, as explained in the following.

When landmark locations are not exactly known they are included among the quantities that must be estimated at each time step. As a consequence, in addition to the robot motion model (1), one has to introduce also a model for the landmarks. If static features are chosen as landmarks, the evolution of their position $l_i(k)$ can be described by the equation

$$l_i(k+1) = l_i(k). \tag{15}$$

Since both robot pose and landmark positions must be estimated, the resulting state estimation problem involves a system whose state dimension can be very large, as it depends on the number of remarkable features present in the environment, which may vary in time. Indeed, when n landmarks are considered, the state vector is given by

$$\xi(k) = [p'(k) \ l_1'(k) \dots l_n'(k)]' \in \mathbb{R}^{(3+2n)}.$$

From equations (1) and (15), the state update equation is

$$\xi(k+1) = \xi(k) + E_3 u(k) + E_3 w(k), \tag{16}$$

where $E_3 = [I_3 \ 0 \dots 0]' \in \mathbb{R}^{(3+2n)\times 3}$.

Concerning the exteroceptive measurements, model (3) is still valid; nonetheless, it must be pointed out that in this case each equation in (4) provides two nonlinear relations among some of the state variables (namely the robot pose and the i-th landmark coordinates). In addition, notice that such measurements provide only relative information: they can be thought of as the displacement of the landmarks with respect to the robot and vice versa.

Under the UBB assumption on the disturbances, the measurement set is still given by (8) where

$$\mathcal{M}_i(k) = \left\{ \xi \in \mathbb{R}^{(3+2n)} : \ |D_i(k) - d(p(k), l_i)| \leq \epsilon^{v_d} \text{ and } |A_i(k) - \alpha(p(k), l_i)| \leq \epsilon^{v_\alpha} \right\}. \tag{17}$$

Notice that $\mathcal{M}_i(k)$ is an unbounded subset of $\mathbb{R}^{(3+2n)}$, because it defines constraints on only five state variables (the other $2n - 2$ being free). According to the hypotheses on the dynamics and

measurement model and on the UBB disturbances assumptions, the localization problem can be formulated as follows.

SM Uncertain Localization Problem: Let $\Xi(0) \subset \mathbb{R}^{(3+2n)}$ be a set containing the initial vehicle pose and landmark positions, $\xi(0)$. Given the dynamic model (16) and the measurement equations (3)-(4), find at each time $k = 1, 2, \dots$ the set $\Xi(k|k)$ of state vectors $\xi(k)$ which are compatible with the robot dynamics, the assumptions (5)-(7) on the disturbances, and the measurements collected up to time k.

The solution to the above problem is still provided by the algorithm outlined in equations (10)-(12), where the robot feasible pose set $P(k)$ is replaced by the extended feasible state set $\Xi(k)$, i.e.

$$\Xi(0|0) = \Xi(0), \tag{18}$$

$$\Xi(k+1|k) = \Xi(k|k) + E_3 u(k) + E_3 \text{Diag}[\epsilon^w] \mathcal{B}_\infty, \tag{19}$$

$$\Xi(k+1|k+1) = \Xi(k+1|k) \cap \mathcal{M}(k+1). \tag{20}$$

The *initialization* step of the algorithm, i.e. the choice of the set $\Xi(0)$, depends on the specific problem tackled. If there is no available information on the initial position of any element of the problem (i.e. robot and landmarks, as it happens in the SLAM case), the initial estimate set $\Xi(0)$ should be chosen as $\mathbb{R}^{(3+2n)}$. Nonetheless, since all measurements are relative, in this case one is allowed to choose an arbitrary reference system. Hence, without loss of generality, it is possible to set the origin of the reference system in the initial position of the robot, choosing as x-axis the robot initial heading. On the other hand, when an uncertain map of the environment is a priori given, $\Xi(0)$ is chosen accordingly to the available information. Clearly, initialization plays a key role, especially in the SLAM case. A possible strategy is that of using a first set of exteroceptive measurements to construct a rough initial map (e.g., by performing a $360°$ scan of the environment in the field of view of the robot), before starting the dynamic recursion (18)-(20).

Notice that in algorithm (18)-(20), equation (19) can be modified in order to account for different models of landmark motion. By using equations similar to (1) to describe landmark dynamics, it is also possible to account for moving landmarks. In (Di Marco, Garulli and Vicino 2001), this is done to tackle the localization problem for a multi-robot system: the single-robot SLAM algorithm above is run as a starting step by each sensing agent, then set-valued information is exchanged and map fusion is performed to achieve cooperative localization.

It is worth remarking that the landmark matching procedure proposed in Section 2.3 can be applied also to the SLAM problem. The only difference is that each landmark l_j is replaced by the corresponding uncertainty set Ξ_{l_j}. If the intersection between such set and the region $\Xi_{xy} + \mathcal{M}_{l_i}$ is not empty (where Ξ_{xy} has the same meaning of P_{xy} in the localization problem), one can associate landmark l_j to the i-th measurement. Ambiguous measurements are defined accordingly.

As observed in Section 2.2, the algorithm solving the set membership pose estimation problem requires the computation of complex sets whose dimension can be considerably high. The exact computation of sums and intersection of non linear, non convex sets is generally a prohibitive task.

Therefore, the main problem consists in devising algorithms suitable for real-time applications that tradeoff between computational complexity and accuracy of the approximations. In particular, approximating sets belonging to a class $\mathcal{R}$ of regions with simple, fixed structure, will be pursued. Section 3 illustrates some general approximation techniques suitable for the solution of the SM localization problems considered in the paper.

3 Set membership algorithm for guaranteed localization

In order to obtain computationally tractable solutions of the SM localization problem, simple approximations of the sets P in (10)-(12) (or Ξ in (18)-(20)) are sought. The choice of the structure and size of the approximating regions $\mathcal{R}$ must be made according to the following criteria:

- recursive updating according to (10)-(12) (or (18)-(20)) must be performed through efficient algorithms, suitable for on-line implementations;

- at each time instant k, the approximating regions $\mathcal{R}(k+1|k)$, $\mathcal{R}(k|k)$ must contain the corresponding exact sets $P(k+1|k)$, $P(k+1|k+1)$ ($\Xi(k+1|k)$, $\Xi(k+1|k+1)$, respectively) so that the true state vector $p(k)$ ($\xi(k)$) is guaranteed to belong to the approximating set.

To satisfy the above requirements, approximations are introduced at different stages of the state estimation procedure:

1. Decomposition of the state vector into subsets of state variables.

2. Guaranteed approximations of the true feasible subsets through classes of simple regions.

We discuss the role of these approximations separately.

3.1 Set membership estimation trough state decomposition

The state vector can be decomposed into different subsets of variables: robot position $(x(k), y(k))$, robot heading $\theta(k)$ and (in the case that the position of the reference features is uncertain) landmark positions $l_i(k)$, $i = 1, \ldots, n$.

Consider the recursion (18)-(20). Let Ξ_{xy} denote the feasible robot position set, Ξ_θ the feasible robot heading set, and Ξ_{l_i} the feasible i-th landmark position set. In addition, let $\Xi_{xy}(0)$, $\Xi_\theta(0)$ and $\Xi_{l_i}(0)$ be the corresponding initial sets (they can be easily obtained by projecting $\Xi(0)$ onto the subspaces defined by (x, y), θ and l_i, respectively). The initialization equation (18) can be decomposed as follows:

$$\Xi_{xy}(0|0) = \Xi_{xy}(0), \quad \Xi_\theta(0|0) = \Xi_\theta(0), \quad \Xi_{l_i}(0|0) = \Xi_{l_i}(0). \tag{21}$$

The time update equation (19) readily boils down to

$$\Xi_{xy}(k+1|k) \;\; = \;\; \Xi_{xy}(k|k) + u_{xy}(k) + \mathrm{Diag}[\epsilon^{w_{xy}}]\mathcal{B}_\infty, \tag{22}$$

$$\Xi_\theta(k+1|k) = \Xi_\theta(k|k) + u_\theta(k) + \text{Diag}[\epsilon^{w_\theta}]\mathcal{B}_\infty, \tag{23}$$

$$\Xi_{l_i}(k+1|k) = \Xi_{l_i}(k|k), \tag{24}$$

The main advantage of state decomposition is obtained in the measurement update step (20), since it allows for sequential update of simple 2D and 1D sets. In principle, these updates can be performed in any order; nonetheless, since distinct subsets are affected differently by the time update, it is possible to devise an order that will generally lead to tighter sets. To do this, the following facts need to be considered:

- Uncertainty on robot heading affects all the measurement uncertainty sets (see equation (13)).

- Bounds on robot heading uncertainty can be evaluated using robot and landmark uncertainty sets and relative orientation measurements. Let us consider the uncertainty sets $\Xi_{xy}(k|k-1)$, $\Xi_{l_i}(k|k-1)$ and the orientation measurement $A_i(k)$. It is easily verified that the sum of the robot heading $\theta(k)$ and the relative orientation $\alpha(p(k), l_i)$ satisfies the constraint

$$\underline{\beta} \le \alpha(p(k), l_i) + \theta(k) \le \overline{\beta},$$

  where

$$\underline{\beta} = \min_{\substack{(x,y)\in\Xi_{xy}(k|k-1) \\ (x_{l_i},y_{l_i})\in\Xi_{l_i}(k|k-1)}} \text{atan}_2(y_{l_i} - y, x_{l_i} - x), \tag{25}$$

  and

$$\overline{\beta} = \max_{\substack{(x,y)\in\Xi_{xy}(k|k-1) \\ (x_{l_i},y_{l_i})\in\Xi_{l_i}(k|k-1)}} \text{atan}_2(y_{l_i} - y, x_{l_i} - x), \tag{26}$$

(see Figure 7). As a consequence,

$$\underline{\beta} - \alpha(p(k), l_i) \le \theta(k) \le \overline{\beta} - \alpha(p(k), l_i). \tag{27}$$

Since only a noisy measurement of $\alpha(p(k), l_i)$ is available, considering the hypothesis (7) on the measurement noise, equation (27) becomes

$$\underline{\beta} - A_i(k) - \epsilon^{v_\alpha} \le \theta(k) \le \overline{\beta} - A_i(k) + \epsilon^{v_\alpha}. \tag{28}$$

Note that equation (28) can be evaluated for each relative orientation measurement, thus providing m intervals, where the true robot orientation is guaranteed to lie.

- Uncertainty on static landmarks does not grow during the time update.

The aforementioned remarks naturally lead to the following approximated measurement update procedure, to be used in place of (20). First, all the orientation measurements at time $k + 1$ are processed in order to reduce the uncertainty on robot orientation (thus allowing for smaller measurement uncertainty sets). From equation (28) one obtains m intervals, $[\underline{\theta}_i, \overline{\theta}_i]$, where the true
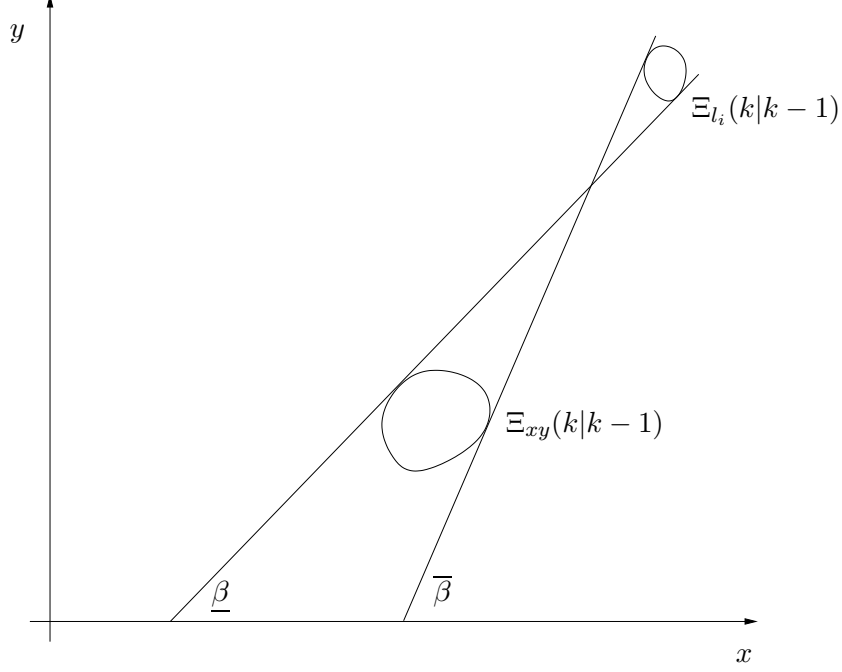
Figure 7: Bounds on robot orientation can be evaluated from the position uncertainty sets and the exteroceptive measurements.

robot orientation is constrained to lie. As a consequence, it is possible to update the robot heading according to

$$\Xi_\theta(k+1|k+1) = \Xi_\theta(k+1|k) \bigcap \left\{ \bigcap_{i=1}^{m} [\underline{\theta}_i, \overline{\theta}_i] \right\}. \tag{29}$$

In the following, we will denote by $\hat{\theta}(k+1)$ the center of $\Xi_\theta(k+1|k+1)$ and by $\epsilon^{\hat{\theta}}(k+1)$ its semi-amplitude.

Now, let us consider robot position. Since each distance and orientation measurement is relative, it is clear that landmark l_i "sees" the robot under the angle $\alpha(p(k+1), l_i(k+1)) + \pi$. It turns out that, using the measurement taken with respect to the i-th landmark and the current robot heading, the position of the vehicle can be written as

$$\begin{cases} x(k+1) = x_{l_i}(k+1) - d(p(k+1), l_i(k+1)) \cos\{\theta(k+1) + \alpha(p(k+1), l_i(k+1))\} \\ y(k+1) = y_{l_i}(k+1) - d(p(k+1), l_i(k+1)) \sin\{\theta(k+1) + \alpha(p(k+1), l_i(k+1))\} \end{cases}. \tag{30}$$

Since $(x_{l_i}, y_{l_i}) \in \Xi_{l_i}(k+1)$, $\theta(k+1) \in \Xi_\theta(k+1|k+1)$, and noises affecting measurements $D_i(k+1)$ and $A_i(k+1)$ are bounded, as assumed in (6)-(7), it turns out that each measurement pair provides a feasible set $\mathcal{C}_{R_i}(k+1)$ where the robot position must lie. This set is given by

$$\mathcal{C}_{R_i}(k+1) = \Xi_{l_i}(k+1|k) + \mathcal{M}_{R_i}(k+1), \tag{31}$$

where

$$\mathcal{M}_{R_i}(k+1) = \big\{ (x,y) \in \mathbb{R}^2 : \ |D_i(k+1) - d(p,0)| \le \epsilon^{v_d} \text{ and } \\ |A_i(k+1) - \mathrm{atan}_2(-y,-x) + \hat{\theta}(k+1)| \le \epsilon^{v_\alpha} + \epsilon^{\hat{\theta}}(k+1) \big\} \tag{32}$$

is the robot position uncertainty set relative to the i-th measurement pair, for a landmark placed at the origin of the reference system. Since this process can be repeated for every detected landmark, the robot position is constrained to lie in the set

$$\mathcal{C}_R(k+1) = \bigcap_{i=1}^{m} \mathcal{C}_{R_i}(k+1). \tag{33}$$

Consequently, it turns out that measurement update for robot position can be performed as

$$\Xi_{xy}(k+1|k+1) = \Xi_{xy}(k+1|k) \bigcap \mathcal{C}_R(k+1). \tag{34}$$

As a third step, we consider again each measurement performed at time $k+1$, this time trying to reduce uncertainty on the landmarks. Note that, since each measurement provides a relationship between sets and no statistical assumption is made, it is possible to use the same measurements to update the uncertainty sets relative to landmarks position. Using an approach similar to the one adopted for robot position, one has that, due to measurements at time $k+1$, the i-th landmark will lie in the set defined by

$$\mathcal{C}_{l_i}(k+1) = \Xi_{xy}(k+1|k+1) + \mathcal{M}_{l_i}(k+1), \tag{35}$$

where

$$\mathcal{M}_{l_i}(k+1) = \big\{ l \in \mathbb{R}^2 : |D_i(k+1) - d(0,l)| \leq \epsilon^{v_d} \text{ and } \\ |A_i(k+1) - \mathrm{atan}_2(y_l, x_l) + \hat{\theta}(k+1)| \leq \epsilon^{v_\alpha} + \epsilon^{\hat{\theta}}(k+1) \big\} \tag{36}$$

is the i-th landmark uncertainty set, for a robot placed at the origin of the reference system. Consequently, measurement update of the i-th landmark position can be performed as

$$\Xi_{l_i}(k+1|k+1) = \Xi_{l_i}(k+1|k) \bigcap \mathcal{C}_{l_i}(k+1). \tag{37}$$

Notice that sets $\mathcal{M}_{R_i}(k)$ and $\mathcal{M}_{l_i}(k)$ are sectors of corona; some examples of $\mathcal{M}_{l_i}(k)$ are shown in Figure 8, while Figure 9 shows how sets $\mathcal{C}_{l_i}$ are computed. Sets $\mathcal{C}_{R_i}(k)$ are obtained through a similar procedure. In addition, Figure 10 reports an example of the second and third step of the measurement update (33)-(37).

Since the evaluation of each set is based on the previously determined approximations, a further refinement of the estimated sets can be achieved by iteratively repeating the three step measurement update. The whole approximated process is summarized in Figure 11. The guiding idea of this approach is similar to the Baum-Welch algorithm (Thrun et al. 1998), where map and robot location are alternatively updated by maximization in the likelihood space. The main difference is that in this case no probabilistic information on the measurements is assumed. Hence, the same measurements are processed several times, in order to iteratively reduce the size of the approximated uncertainty sets. Heuristic criteria can be formulated to stop the recursion in Figure 11. In practice, very few iterations are generally sufficient to significantly reduce the size of the uncertainty sets.

The proposed approach allows one to simplify the measurement update process, but it also introduces an approximation because information about correlation between robot and landmark
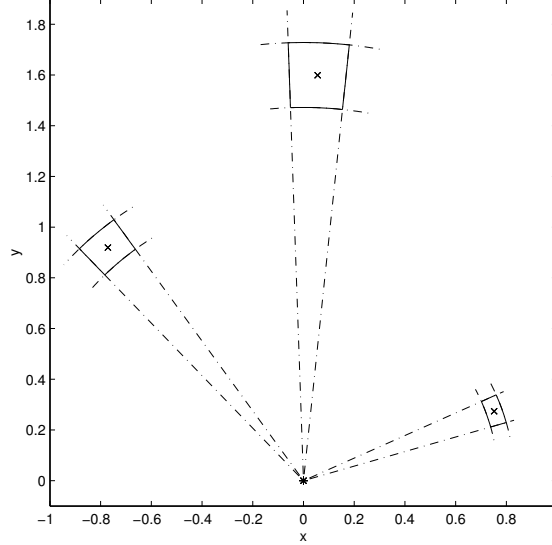
Figure 8: Examples of landmark uncertainty sets associated to distance and relative orientation uncertain measurements (∗: robot position; ×: nominal landmark position).

PSfrag replacements

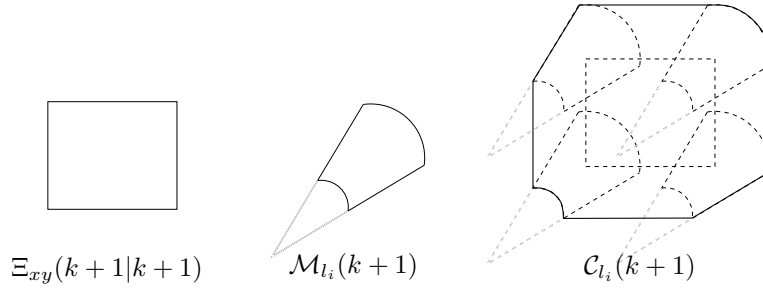$$\Xi_{xy}(k+1|k+1) \qquad \mathcal{M}_{l_i}(k+1) \qquad \mathcal{C}_{l_i}(k+1)$$

Figure 9: Example of set $\mathcal{C}_{l_i}$, given by the sum of sets $\Xi_{xy}(k+1|k+1)$ and $\mathcal{M}_{l_i}(k+1)$.

position is lost. Indeed, the approximated measurement update described in this section is more conservative than the original set membership algorithm presented in Sections 2.2 and 2.4, where only the state vectors satisfying equations (19)-(20) are deemed feasible for $\Xi(k|k)$. On the other hand, notice that the set

$$\Xi_{xy}(k|k) \otimes \Xi_{\theta}(k|k) \otimes \Xi_{l_1}(k|k) \otimes \ldots \otimes \Xi_{l_n}(k|k),$$

where $\otimes$ denotes the Cartesian product, is guaranteed to include the true feasible set $\Xi(k|k)$, and hence to contain the actual robot pose and landmark positions.

3.2 Set approximation

Computing exact sums and intersections of nonconvex regions bounded by nonlinear curves, as required by the aforementioned approximated measurement update procedure, implies a high computational burden. Since we are interested in fast algorithms, which are able to provide regions
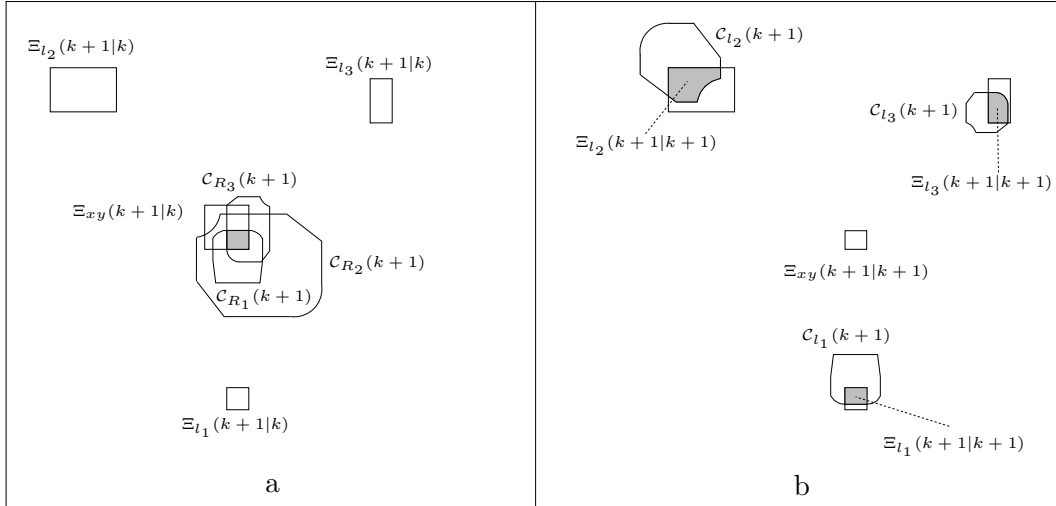
Figure 10: Example of second and third step of the approximated measurement update procedure: a) robot position update, (dashed region is $\Xi_{xy}(k+1|k+1)$ given by (34)) b) landmark position update (dashed sets are $\Xi_{l_i}(k+1|k+1)$ given by (37)).

guaranteed to contain the robot pose and landmark positions, outer approximations of the feasible sets will be looked for. The approximating sets will belong to classes of simple structure sets. The choice of the specific element in the approximating class must be performed according to some criterion. Since one is usually interested in reducing as much as possible the size of the uncertainty affecting the estimated positions, minimum area sets in the chosen class containing $\Xi_{xy}(k+1|k)$, $\Xi_{xy}(k+1|k+1)$ and $\Xi_{l_i}(k+1|k+1)$ will be selected.

Let us consider a class of regions $\mathcal{R}$ of fixed structure, and let us denote by $\overline{\mathcal{R}}\{\mathcal{Z}\}$ the minimum volume set in the class $\mathcal{R}$ containing the set $\mathcal{Z}$. For the general set membership localization procedure described by (18)-(20), the desired outer approximation is given by the following recursion

$$\mathcal{R}(0|0) = \overline{\mathcal{R}}\{\Xi(0)\} \tag{38}$$

$$\mathcal{R}(k+1|k) = \overline{\mathcal{R}}\{\mathcal{R}(k|k) + E_3 u(k) + E_3 \text{Diag}\{\epsilon^w\}\mathcal{B}_\infty\} \tag{39}$$

$$\mathcal{R}(k+1|k+1) = \overline{\mathcal{R}}\{\mathcal{R}(k+1|k) \cap \mathcal{M}(k+1)\} \tag{40}$$

i.e., by computing the minimum volume element $\overline{\mathcal{R}}$ in the class $\mathcal{R}$ for each step of the proposed algorithm. Notice that, with the introduction of the approximating class, all the set operations in (38)-(40) are now performed on sets of known and simple structure. The proposed approximation algorithm can be applied together with the state decomposition proposed in Section 3.1: in this case, the desired approximation is obtained by computing $\overline{\mathcal{R}}$ for each set in the right-hand side of equations (21)-(24), (29), (34) and (37).

The choice of the class $\mathcal{R}$ of approximating regions is performed taking into account the trade-off between accuracy and computational complexity. As it has been outlined in the previous section, for each step of the set membership localization algorithm, several computations need to be performed
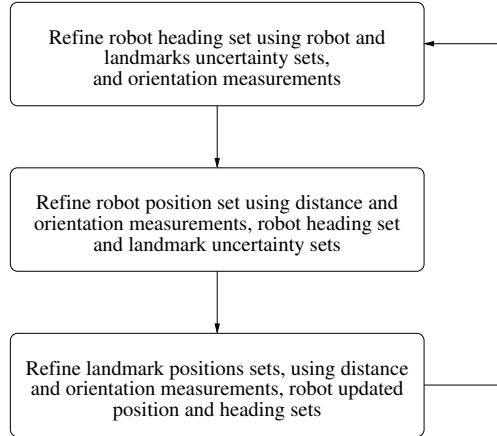
Figure 11: Modified measurement update step, after state decomposition, for the SM uncertain localization problem.

on the uncertainty sets (sums, intersections, minimization of suitable functions). Common choices found in the literature are ellipsoids (Deller, Nayeri and Odeh 1993), orthotopes (axis aligned boxes) (Pshenichnyi and Pokotilo 1983) and parallelotopes (Chisci, Garulli, Vicino and Zappa 1998). More specifically, let us consider the last two classes of sets. The following results are available:

1. From set membership linear estimation theory, fast approximated algorithms performing set sums and outer approximations required by (39), are given in (Garulli and Vicino 2001, Chisci, Garulli and Zappa 1996, Vicino and Zappa 1996).

2. The computation of the intersection of the approximated state space set $\mathcal{R}(k + 1|k)$ with the measurement set $\mathcal{M}(k + 1)$ strongly depends on the choice of the sensors, since different kinds of sensors provide differently shaped sets (cf. Figures 2-3). As a matter of fact, in order to have computationally tractable problems, state decomposition has to be employed. Algorithms providing approximations of the sets described in equations (34) and (37) have been developed for angular distance measurements (Garulli and Vicino 2001) and for the pair distance-angle measurements (3) (Di Marco et al. 2000).

3. Concerning the problem of finding bounds on robot orientation θ, as required by equations (28)-(29), we point out that, when orthotopes or parallelotopes are employed as approximating sets, the extrema defined in (25) and (26) are reached when both the robot and landmark position lie in one of the vertices of those sets. Consequently, the two aforementioned optimization problems boil down to evaluating the function atan_2 on a finite number of points (16, if 2D orthotopic or parallelotopic set approximations are employed).

These results allow one to obtain computationally efficient algorithms which provide guaranteed set-valued solutions to the SM localization problem.

3.3 Computational complexity

It is interesting to analyze the computational complexity of the proposed SM localization procedures. With respect to the number of landmarks, the algorithms perform a fixed number of operations for each measurement pair, i.e. for each of the m landmarks detected and correctly associated to the corresponding measurements, at time k. Since $m \leq n$ (the total number of landmarks), the complexity at each time step is at most $O(n)$. Clearly, if n is large and fast robot dynamics are required, one can restrict the maximum number of landmarks actually processed at each measurement update to a prescribed number $\bar{m}$, thus limiting complexity to $O(\bar{m})$.

It is also worth performing a deeper complexity analysis, in terms of low-level operations that the localization algorithm has to perform at each time k. Thanks to state decomposition, the basic tasks of the algorithm are approximations of 2D regions via simple sets like boxes or parallelotopes (a typical example being the computation of the minimum area box containing the intersection between a box and the region $\mathcal{C}_{l_i}$, as required by the approximation of equation (37) through boxes). Efficient algorithms for performing these approximations have been reviewed in Section 3.2 and require very few simple algebraic operations. For this reason, we will denote them as Elementary Set Updates (ESU) in the following. At time k, m landmarks are detected and a measurement pair D_i, A_i is performed for each landmark. Each measurement pair corresponds to one elementary region $\mathcal{M}_{R_i}$ (or $\mathcal{M}_{l_i}$). If the procedure outlined in Section 3.1 is adopted, each measurement pair is processed twice: once for robot position update (31)-(34) and once for landmark position update (35)-(37). Moreover, orientation measurements D_i are used also for updating uncertainty on robot heading, according to (29). Therefore, $3m$ ESUs are performed at time k. If the procedure is iterated ρ times, according to the scheme in Figure 11, one has that $3\rho m$ ESUs are required. Hence, $3\rho n$ is the maximum number of ESUs that the localization algorithm must perform at each time step. Notice that ρ is a tuning parameter that can be used to trade-off computational complexity and quality of the approximations (i.e., localization precision).

4 Experimental testing

In this section, results from both numerical simulations and experimental tests are presented.

4.1 Numerical simulations

In order to get a quantitative evaluation of the proposed localization algorithm, extensive simulations have been performed. First, a static setting has been considered. At a fixed time $k = 0$, the vehicle is supposed to lie at the center of a square room of 20 meters size, having no a priori information on its pose. Under these assumptions, the true vehicle pose is $p(0) = [0\ 0\ 0]'$ in a robot centered reference system and $\mathcal{R}(0|-1)$ is a 3D box of sides $10\,m$, $10\,m$ and $180°$, respectively. The robot is able to correctly identify a certain number of known landmarks present in the surrounding environment and to collect angular and distance measurements with respect to these features.

Such measurements are corrupted by additive noises $v_{d_i}(k)$ and $v_{\alpha_i}(k)$ generated as independent uniformly distributed (i.u.d.) signals satisfying (6) and (7). Assuming as nominal pose estimate the center of the box $\mathcal{R}(0|0)$, the estimation error and the size of the associated uncertainty region, have been computed for different values of ϵ^{v_d} and ϵ^{v_α} ranging from 0.05 to 0.25 meters and from $0.5°$ to $2.5°$, respectively. In Figure 12 these quantities, averaged over 1000 different landmark configurations, are reported for 5 known landmarks.
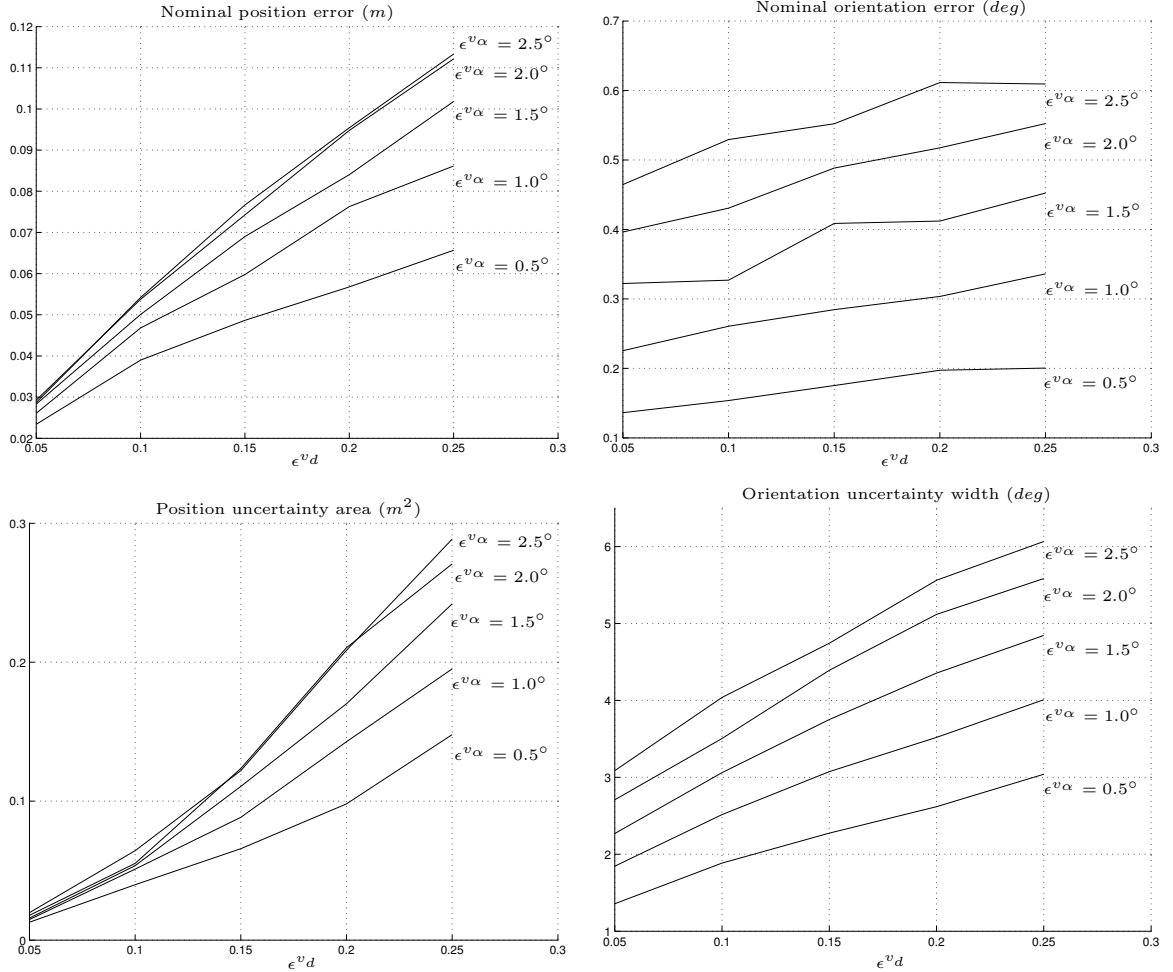

Figure 12: Static simulation results with 5 known landmarks.

Another set of simulation experiments has been performed to evaluate the performances of the SLAM algorithm. The robot moves in a square room of about $50\,m^2$ area, where a number of landmarks is randomly spread. The robot is not able to detect landmarks which are farther than 6 meters, and it does not have any initial information on landmark positions. While the robot moves in the room, it builds a map centered in its own initial position. Tables 1a-1b report the simulation results, averaged over 25 experiments, for different numbers of landmarks present in the scene. In the experiments reported in the Table 1a, all the noises are i.u.d. with $\epsilon^{v_d} = 0.1\,m$ and $\epsilon^{v_\alpha} = 2.5°$. The bounds on the errors affecting odometric sensors are supposed to be essentially

proportional to the nominal relative displacement, $\epsilon^w(k) = 0.05|u(k)| + \delta$, $\delta = [0.02m\ 0.02m\ 1°]'$, with δ accounting for possible errors along nominal steady axes. In Table 1b, noises have been generated according to truncated Gaussian distributions, with standard deviation σ chosen such that 3σ equals the above mentioned bounds. Note that the behavior of the algorithm is similar in the two cases. Nevertheless, when measurements are affected by uniformly distributed noises, the nominal errors are larger than in the case of Gaussian noises, while the uncertainty bounds are tighter. This is in accordance with the theory of set membership estimation, which delivers smaller uncertainty regions when "boundary visiting" noises affect the measurements.

Uniformly distributed disturbances						
N_{land}	NPE	PUA	NLE	ALUA	NOE	OUW	ADL
5	0.075	0.269	0.083	0.194	1.966	15.986	4.449
7	0.069	0.214	0.087	0.165	1.133	16.630	6.212
10	0.059	0.186	0.078	0.153	0.982	13.593	8.952
15	0.055	0.115	0.071	0.108	0.926	10.658	13.818
20	0.049	0.101	0.068	0.112	0.860	9.873	17.673

(a)

Gaussian disturbances						
N_{land}	NPE	PUA	NLE	ALUA	NOE	OUW	ADL
5	0.069	0.346	0.066	0.335	1.692	18.233	4.362
7	0.065	0.269	0.058	0.198	0.852	16.152	6.219
10	0.057	0.234	0.053	0.184	0.742	14.866	8.842
15	0.049	0.206	0.055	0.199	0.708	14.155	13.358
20	0.045	0.183	0.052	0.191	0.549	13.563	17.706

(b)

Table 1: Results from simulation experiments performed on the SLAM algorithm. N_{land}: number of landmarks present in the room, NPE: nominal robot position error (m), PUA: robot position uncertainty area (m^2), NLE: nominal landmark position error (m), ALUA: average landmarks uncertainty area (m^2), NOE: nominal robot orientation error (deg), OUW: orientation uncertainty width (deg), ADL: average number of detected landmarks at each measurement scan.

4.2 Comparison with Kalman filter

In Sections 2.1 and 2.4, it has been pointed out that both the localization and the SLAM problems can be cast as the state estimation of a dynamical system. Therefore, the Kalman filter represents a natural way of addressing the problem. Being the measurement process (3)-(4) nonlinear, the

Extended Kalman Filter (EKF) must be employed.

In this section, the performance of the SM technique is compared to that of an EKF-based algorithm. Specifically, both nominal estimation errors and estimation uncertainties are taken into account. To this purpose, several simulations were run, with different number and configuration of landmarks. All the results are averaged over 100 different noise realizations.

A crucial issue, for the comparison to be fair, is the choice of the tuning parameters of the EKF, i.e. the matrices $\mathbf{Q}$ and $\mathbf{R}$ representing process disturbance and measurement error covariances, respectively. The theoretical values of noise covariances will be used, unless otherwise specified.

The scenario of the tests is similar to the one outlined in Section 4.1: the robot covers rough square paths in environments where a certain number of landmarks are spread. Depending on the problem considered, landmark positions are supposed to be known (localization problem) or they are quantities to be estimated (SLAM problem).

Both proprioceptive and exteroceptive measurements are corrupted by additive noises generated as i.u.d. signals satisfying (5)-(7), with $\epsilon^{v_d} = 0.2m$, $\epsilon^{v_\alpha} = 2.5°$ and $\epsilon^w(k) = 0.05|u(k)| + \delta$, $\delta = [0.02m\ 0.02m\ 1°]'$.

For each set of simulations, the errors on robot position and orientation (and on landmark position, in the SLAM case) of the estimates delivered by the EKF are compared to the errors provided by the SM algorithm (the nominal estimates being computed as in Section 4.1). The Kalman filter provides both the state estimate $\hat{\xi}(k|k)$ and the covariance matrix $P(k|k)$ of the estimation error $\tilde{\xi}(k|k) = \xi(k|k) - \hat{\xi}(k|k)$. For white Gaussian noises and linear models, this information allows one to compute confidence ellipsoids with a given probability of containing the actual state vector.[1] The area of the 99% confidence ellipses for robot position (and for landmark position, in the SLAM case) and the width of the 99% confidence interval for robot orientation, are compared to the size of the corresponding guaranteed uncertainty regions, as computed by the SM algorithm.

Figures 13a and 13b show the results of the comparison, for localization with 5 known landmarks. Both techniques exhibit comparable performance, in terms of nominal estimation error and estimation uncertainty. The SM algorithm seems to better estimate robot orientation, while the EKF shows a smaller robot position error. Note that the spikes in the width of the 99% confidence intervals of orientation estimation are due to the proportional nature of the errors affecting odometry: when the vehicle reaches a corner of the square path and makes a 90° rotation, the information on relative orientation movement, provided by encoders, is supposed to be significantly more noisy than the one gathered along the edges of the nominal trajectory.

To evaluate the transient behavior of the localization algorithms, a set of simulations was carried out in which the initial estimate of vehicle position is set 3 meters away from the true one. In the SM approach, the inaccuracy of the a priori knowledge is taken into account by the initial uncertainty

---

[1] Note that in the setting considered here the assumptions of model linearity and Gaussian disturbances are not satisfied. Therefore, $\tilde{\xi}(k|k)'P^{-1}(k|k)\tilde{\xi}(k|k)$ is not a χ^2 distributed random variable with n degrees of freedom. Nonetheless, confidence ellipsoids are a standard way of evaluating the quality of the estimate, thus being a suitable tool for comparison purposes.
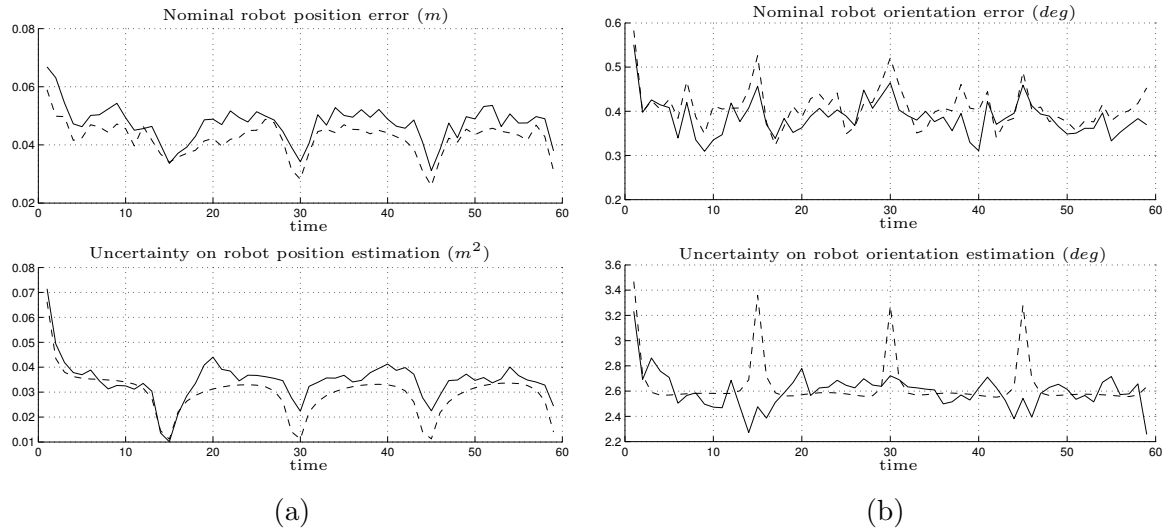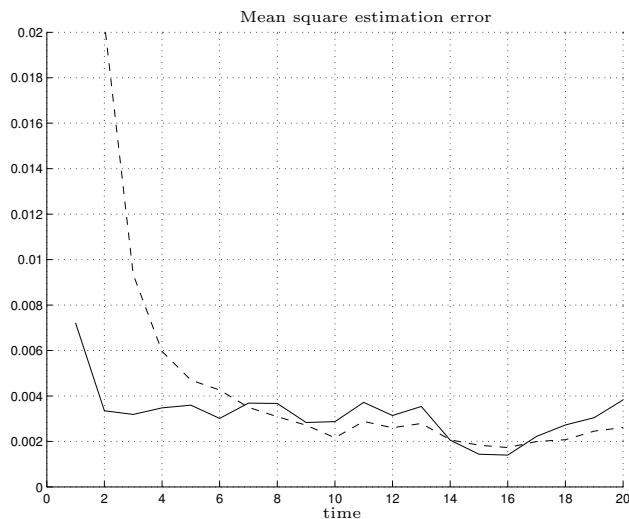
Figure 13: Comparison between SM (solid lines) and EKF (dashed lines) for a localization problem with 5 landmarks: nominal robot position errors and area of uncertainty regions (a), nominal robot orientation errors and width of uncertainty intervals (b).

region $\mathcal{R}(0|-1)$, while the EKF includes this information in the initial covariance matrix $P(0|-1)$. Choosing the initial robot $x-y$ coordinates as i.u.d. random variables in an interval of 10 meters width centered at the initial estimate, and the robot orientation u.d. in $[-\pi,\ \pi)$, $P(0|-1)$ is set as a diagonal matrix with $[25/3\ 25/3\ \pi^2/3]$ on its diagonal.

Figure 14: Comparison between SM (solid lines) and EKF (dashed lines) for a localization problem with 5 landmarks: transient response.

The mean square error of the robot pose estimation is depicted in Figure 14. The SM algorithm clearly exhibits a better transient response. As a matter of fact, just the first collected exteroceptive measurements are necessary to correct the poor initial estimate, while the error made by the EKF

reaches its steady state value after about 6 measurements. This property of the SM approach turns out to be very useful not only at the beginning of a robot localization run, but whenever the estimation error (and the corresponding estimation uncertainty) experiences a significant increase (e.g. because of temporary measurement unavailability, due to transient sensor faults or lack of landmarks in sight).

Other simulations were aimed to assess the performance of the deterministic and statistical approaches in presence of slightly time-correlated bounded noise (see Figure 15).

PSfrag replacements
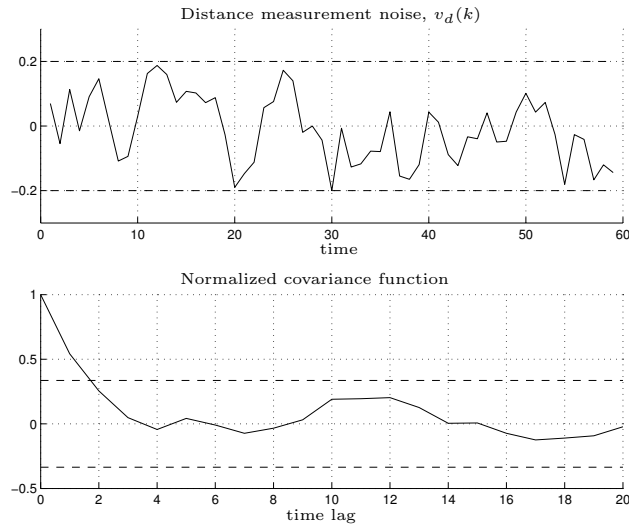
Figure 15: Correlated noise. Top: a typical realization. Bottom: estimated covariance function and corresponding whiteness test bounds.

Not surprisingly, these simulations reveal an increase of nominal errors for both techniques (actually, more evident in the EKF) with respect to the white noise scenario, while the estimation uncertainty remains basically the same. More interestingly, about 11% of the the true robot positions lie outside the 99% confidence ellipses computed by the EKF (while, by construction, the true robot state always belongs to the uncertainty regions computed by SM algorithm). This observation suggests that, under these conditions, the EKF tends to overrate the quality of its estimates. Such conjecture is supported by the comparison of the actual mean square error and the one predicted by the filter (see Figure 16). A typical way to preserve the consistency of the estimate is to suitably *tune* the EKF by enlarging the noise covariance matrices $\mathbf{Q}$ and $\mathbf{R}$. Accordingly, new experiments were performed by increasing $\mathbf{Q}$ and $\mathbf{R}$ until no more than 1% of true robot positions be outside the EKF 99% confidence ellipses. The results, summarized in Figures 17a and 17b, show the better performance of SM algorithm, especially in terms of estimation uncertainty.

Analogously to the localization problem, also the SM and EKF techniques have been compared via numerical simulations on the SLAM problem. In this case, the dimension of the state to be estimated dynamically grows, in order to encompass also the position of the landmarks present in the surrounding environment. The exteroceptive sensors the robot is equipped with are supposed to have a limited field of view (specifically, they are not able to sense landmarks farther than 8
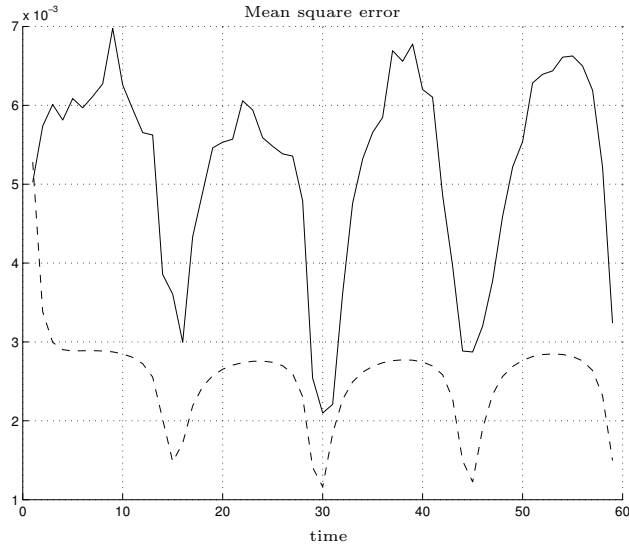
Figure 16: Actual (solid line) and predicted by EKF (dashed line) mean square error, in presence of correlated noise.

meters from the current vehicle location). During the exploration, the robot incrementally detects new features and updates the map. As mentioned in Section 2.4, the estimate of the initial robot pose can be fixed arbitrarily and the corresponding uncertainty is set to zero (i.e., the map is built in a reference system centered at the initial vehicle configuration). Since a key performance index for such a problem is the quality of the constructed map, the comparison is focused on the nominal error and the associated uncertainty of the final landmark position estimates.

The robot explores an area of about 300 m^2 where 9 landmarks are present. All noises are i.u.d. signals bounded as described at the beginning of this Section. When the theoretical noise variances are used, even with white noises, the EKF delivers inconsistent estimates: 18% of robot position and 34% of final landmark position estimates were found to be outside the corresponding 99% confidence ellipses. Of course, such behavior is even more remarkable in presence of correlated disturbances. Tuning the filter covariances so that no more than 3% of final landmark positions lie outside the associated confidence ellipse, leads to the results summarized in Figures 18-19. Concerning the final maps built by the two algorithms, the SM approach provides tighter uncertainty regions for the landmark positions, the average nominal error of the estimates being comparable. Concerning the robot pose, the estimates provided by EKF exhibit smaller nominal estimation error but are affected by higher uncertainty. [2]

This comparison shows that the SM approach represents a valuable alternative to statistical localization and map building methods whenever the bounded error assumption is verified. A major advantage of the SM SLAM algorithm lies in its reduced computational burden (see Section 3.3)

---

[2]The uncertainty on the EKF robot pose estimates is probably overestimated, since the filter was tuned basically to guarantee a 97% confidence level of landmark position estimates. Different choices of $\mathbf{Q}$ and $\mathbf{R}$ lead to smaller robot uncertainty at the price of less reliable information on the quality of landmark position estimates.
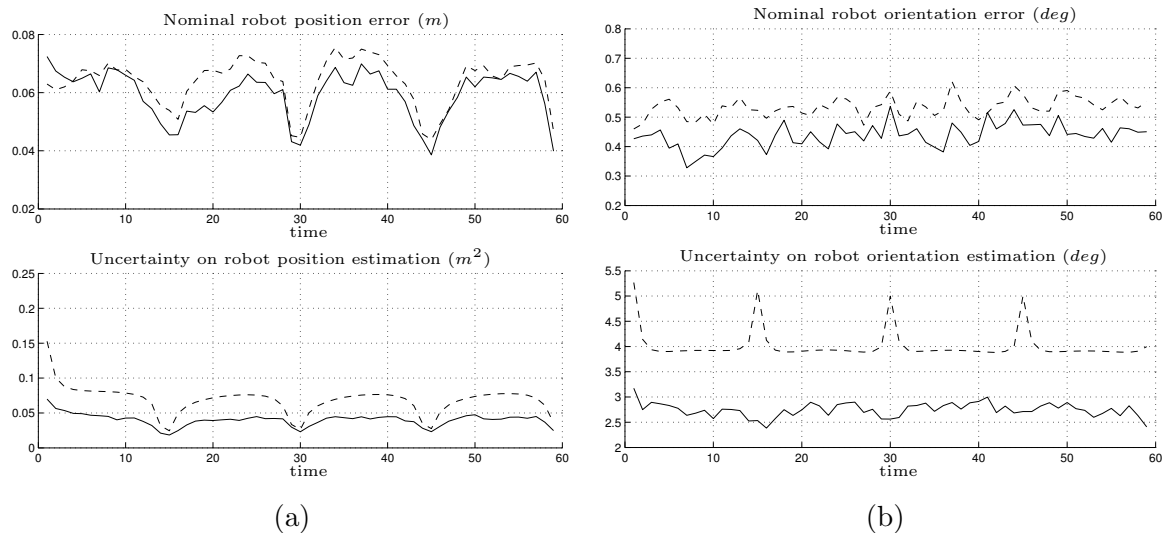
Figure 17: Comparison between SM (solid lines) and tuned EKF (dashed lines) for a localization problem with 5 landmarks: nominal robot position errors and area of uncertainty regions (a), nominal robot orientation errors and width of uncertainty intervals (b).

and memory requirements ($O(n)$ as opposed to $O(n^2)$ for EKF). Such a feature is of paramount importance when exploring large areas (and consequently detecting a large number of landmarks). At each step, the SM algorithm performs a number of operation proportional to the number of currently sensed landmark, whereas the EKF requires the propagation of the whole covariance matrix (a very expensive task when the number of landmarks increases). Moreover, the suboptimal solution devised (based on state decomposition and set approximation), although introducing some conservativeness, provides state estimates whose uncertainty is often smaller than the corresponding one computed by the EKF (especially in case of non Gaussian, non white noise).

4.3 Experimental results

The proposed localization technique has been tested in a laboratory setup featuring the mobile robot Nomad XR4000. This vehicle has a holonomic drive system and is equipped with a SICK LMS 200 laser rangefinder, whose scanning angle width is $180°$ with a resolution of $0.5°$.

The robot was programmed to follow a nominal path in an empty room with 10 artificial landmarks (see Figure 20), using only information provided by the encoders. Periodically, laser scans of the environment were taken in order to estimate the vehicle pose. The signal provided by the rangefinder was first processed by a derivative filter and then compared to a threshold (see Figure 21). By properly setting the threshold value, it was possible to reliably detect the presence of landmarks. As a byproduct of this feature extraction phase, bounds ϵ^{v_α} on the angular measurement error were obtained. Afterwards, the collected measurements were associated to the respective landmarks according to the procedure presented in Section 2.3. Exploiting the guaranteed uncertainty region of
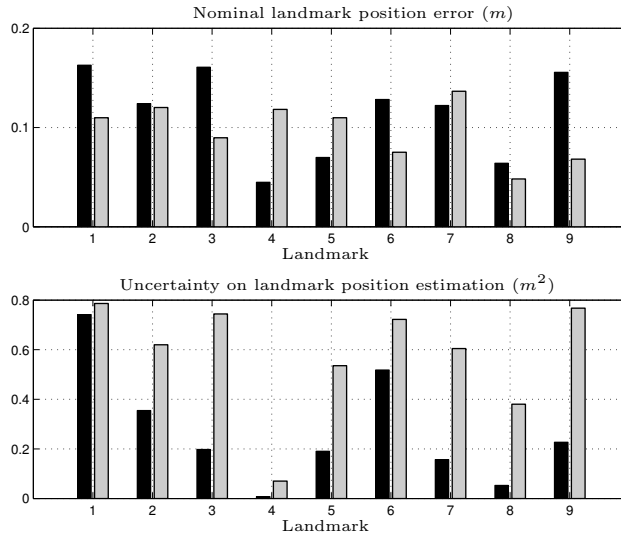
Figure 18: Comparison between SM (black) and tuned EKF (gray) for a SLAM problem with 9 landmarks: final nominal landmark position error (top) and area of uncertainty regions (bottom).

the vehicle configuration (and of the landmarks position, in the SLAM case), the proposed strategy allowed to find the correct matching even in cases in which ambiguous measurements were present. Finally, the robot pose uncertainty set (and the landmark uncertainty sets, for the SLAM problem) was updated using the localization technique in Section 3. The overall measurement update step is summarized in Figure 22, where the *Map building* module handles map updating in the SLAM problem.

In Figure 23 the results of a typical experiment, with known landmarks, are shown. The odometry error bound was set to $\epsilon^w(k) = 0.05|u(k)| + [0.08\ 0.08\ 1°]'$, while $\epsilon^{vd} = 0.05\,m$ was used as distance measurement error bound (from the rangefinder data sheet).

To allow for initial landmark matching, a bounded region for the initial pose was used, assuming $\mathcal{R}(0)$ equal to a 3D box of sides $1\,m$, $1\,m$ and $10°$, respectively.

To evaluate the performances of the proposed algorithm, three trajectories are considered: the nominal one, provided by the odometers, the one provided by the proposed algorithm, and a "true" trajectory, obtained by processing multiple measurements for each landmark, at each robot move. As expected, the true trajectory (solid line) followed by the vehicle rapidly drifts away from the nominal one (dashed line), due to error accumulation typical of odometric sensors. On the other hand, the SM algorithm provides an accurate estimate of the vehicle pose. The estimated trajectory (dash-dotted line, nearly invisible in Figure 23a) is almost indistinguishable from the true one, with an average position and heading error less than $2\,cm$ and $0.1°$. Moreover, the associated uncertainty regions are very small, with average values of $0.016\,m^2$ and $3.4°$ for position and orientation, respectively, in good agreement with the simulation results. Notice that the nominal trajectory is often outside the estimated feasible set (see Figure 23b).

Similar experiments were repeated for the SLAM problem (see Figure 24). Even without any a

Sfrag replacements   PSfrag replacements

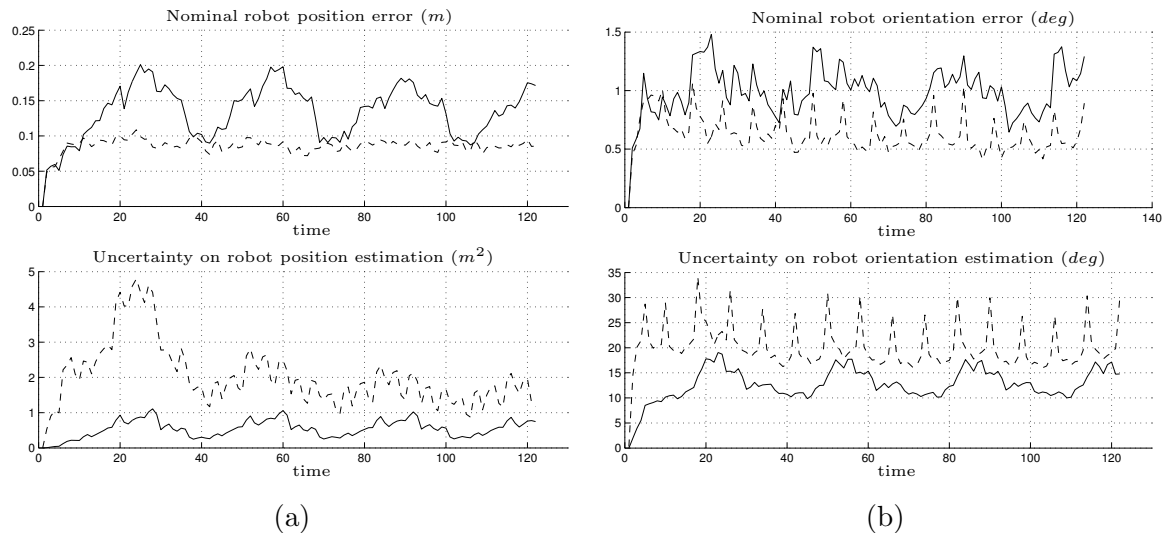(a)   (b)

Figure 19: Comparison between SM (solid lines) and tuned EKF (dashed lines) for a SLAM problem with 9 landmarks: nominal robot position errors and area of uncertainty regions (a), nominal robot orientation errors and width of uncertainty intervals (b).

priori map, the proposed localization algorithm exhibits a good behavior, providing an estimated trajectory quite close to the true one, with average position and heading errors equal to $7\,cm$ and $1.2°$, respectively. Clearly, the lack of a priori information on the surrounding environment causes an increase of the average robot position and orientation uncertainty regions, equal to $0.11\,m^2$ and $8°$, respectively. Landmark positions are estimated with an average nominal error of $7\,cm$ and an associated uncertainty region of $0.13\,m^2$.

Notice that, due to the kind of sensor used to extract environment information, only a $180°$ scan of the surrounding environment was visible to the vehicle at a given time. This means that at each measurement step only a subset of the landmarks was detected. Nevertheless, the matching strategy employed turned out to be very effective, allowing every extracted landmark to be correctly identified and available to the localization procedure.

Concerning the computational burden, a non-optimized Matlab code performing a typical localization step in presence of 7 landmarks (consisting of a time-update and a measurement-update as in Figure 22, iterating twice the refinement procedure in Figure 11), took about $0.1\,s$ on a $1.3\,GHz$ Athlon processor, thus confirming the suitability of this technique for on-line implementation.

5   Conclusions

In this paper, a set-theoretic approach to mobile robot localization has been introduced, analyzed and validated via numerical simulations and experimental testing. The approach is able to cope with both localization based on a given map and the much harder SLAM problem.

The use of indistinguishable landmarks is possible, thanks to the set membership uncertainty
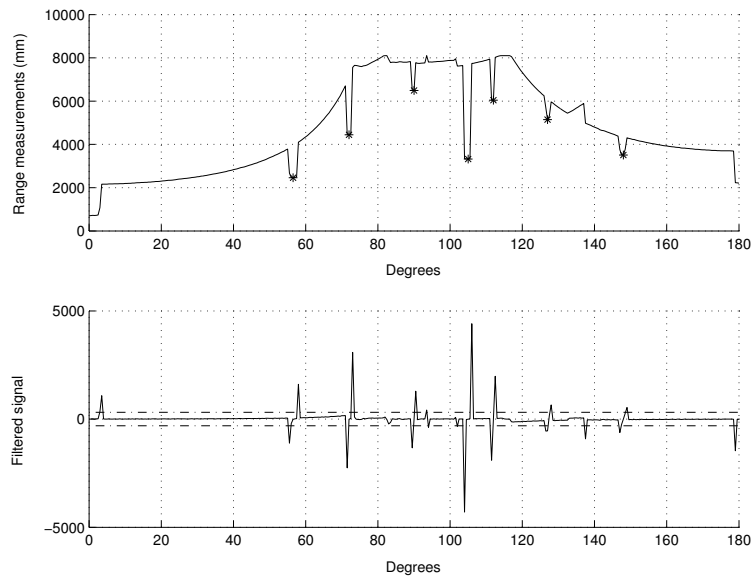
Figure 20: Experimental setup.

Figure 21: A typical laser scan (top) and the corresponding filtered signal (bottom).
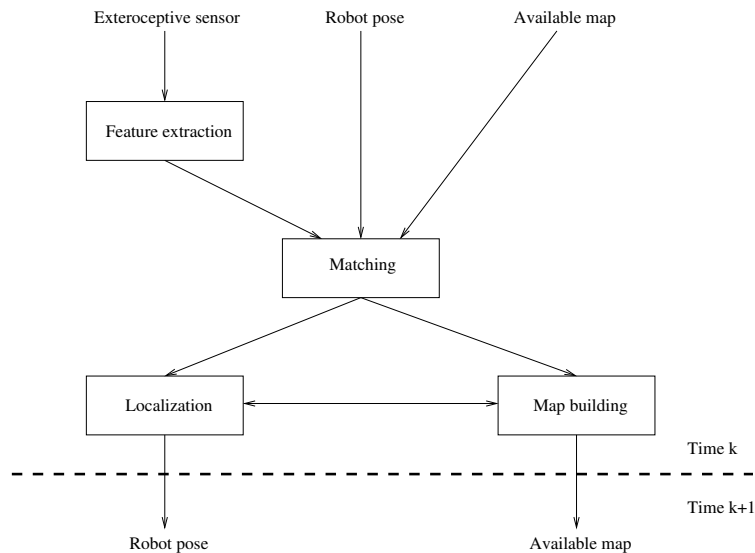
Figure 22: Measurement update.

representation which allows the robot to associate each collected measurement to the corresponding landmark. Efficient set approximation techniques exploiting the specific geometry of the involved sets lead to limited complexity localization algorithms which proved to be effective in real-time experiments.

Ongoing research concerns the use of set membership techniques to tackle some of the most significant hard challenges in autonomous mobile robotics, like cooperative SLAM for a team of agents with different sensing equipments and coordinate motion planning based on set-valued uncertainty representation.

References

Atiya, S. and Hager, G. D.: 1993, Real-time vision-based robot localization, *IEEE Trans. on Robotics and Automation* **9**(6), 785–800.

Barshan, B. and Durrant-Whyte, H. F.: 1995, Inertial navigation systems for mobile robots, *IEEE Transactions on Robotics and Automation* **11**(3), 328–342.

Betke, M. and Gurvits, L.: 1997, Mobile robot localization using landmarks, *IEEE Transactions on Robotics and Automation* **13**(2), 251–263.

Brooks, R. A.: 1986, Robust layered control system for a mobile robot, *IEEE Trans. Robotics and Automation* **2**(1), 14–23.

Castellanos, J. A. and Tardos, J. D.: 1999, *Mobile Robot Localization and Map Building: A Multi-sensor Fusion Approach*, Kluwer Academic Publisher, Boston.
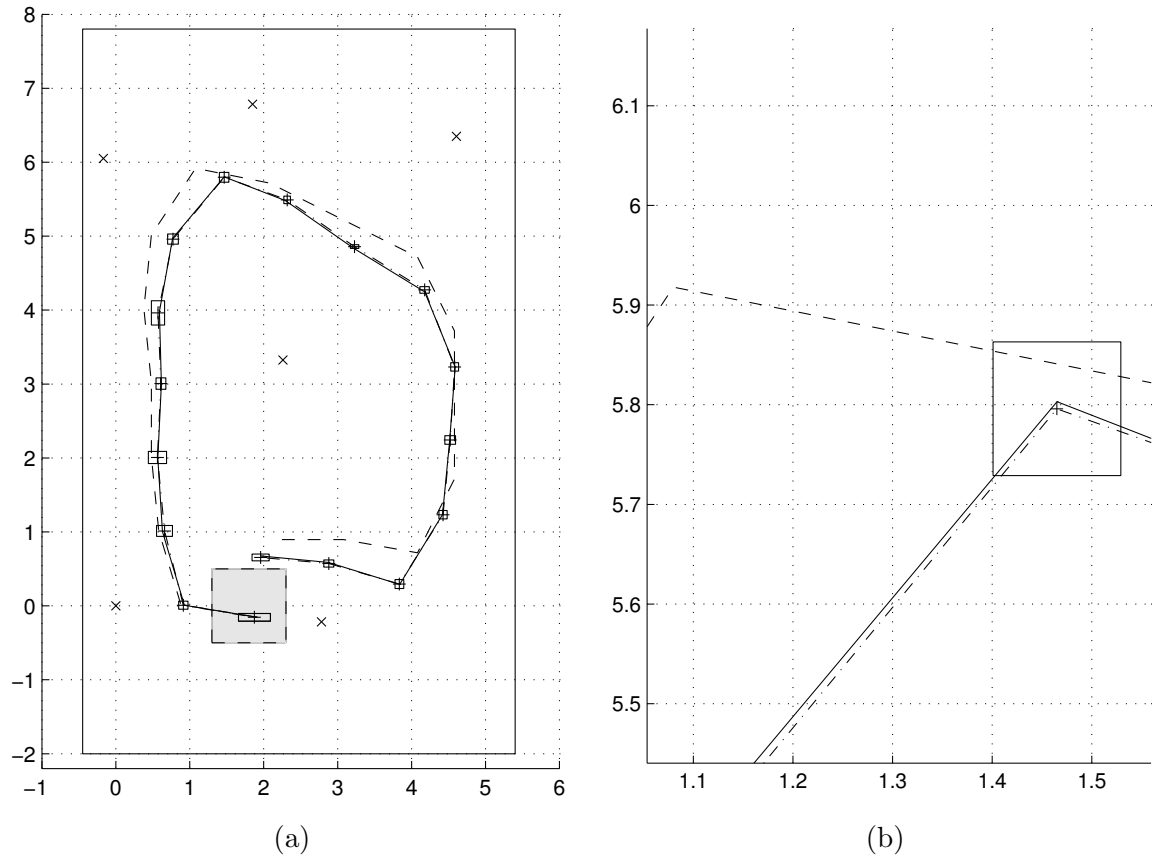
Figure 23: Experimental results with 6 *known* landmarks (x): (a) nominal trajectory (dashed line), true trajectory (solid line), estimated trajectory (dash-dotted line); (b) magnified view of the top of the path, with position uncertainty region (box).

Chisci, L., Garulli, A., Vicino, A. and Zappa, G.: 1998, Block recursive parallelotopic bounding in set membership identification, *Automatica* **34**, 15–22.

Chisci, L., Garulli, A. and Zappa, G.: 1996, Recursive state bounding by parallelotopes, *Automatica* **32**, 1049–1055.

Cox, I. J.: 1991, Blanche - an experiment in guidance and navigation of an autonomous mobile robot, *IEEE Transactions on Robotics and Automation* **7**(3), 193–204.

Deller, J. R. J., Nayeri, M. and Odeh, S. F.: 1993, Least-square identification with error bounds for real-time signal processing and control, *Proceedings of the IEEE* **81**, 815–849.

Di Marco, M., Garulli, A., Lacroix, S. and Vicino, A.: 2000, A set theoretic approach to the simultaneous localization and map building problem, *IEEE Conference on Decision and Control*, Sidney, pp. 833–838.
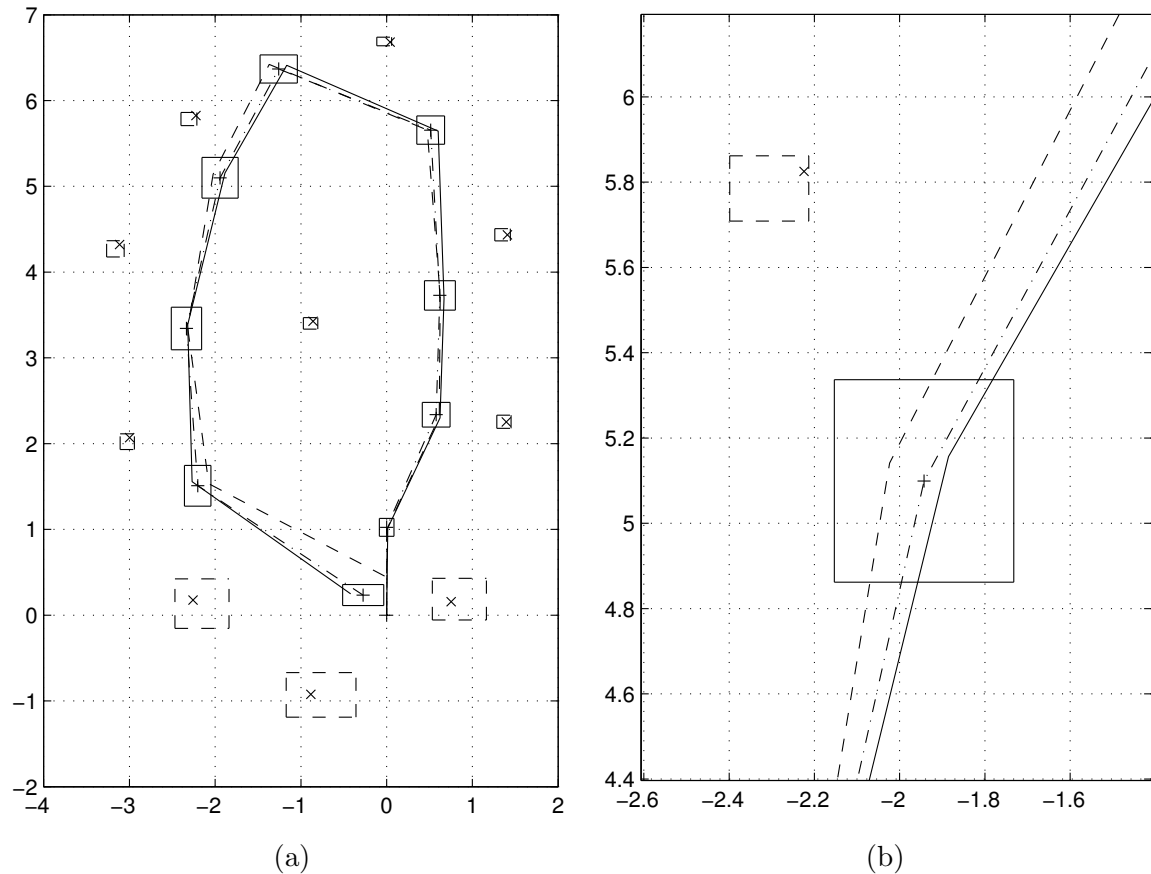
Figure 24: Experimental results with 10 *unknown* landmarks (x): (a) nominal trajectory (dashed line), true trajectory (solid line), estimated trajectory (dash-dotted line); (b) magnified view of left-bottom of the path, with robot (solid box) and landmarks (dashed box) position uncertainty region.

Di Marco, M., Garulli, A. and Vicino, A.: 2001, Cooperative localization and map building for multi-robot systems: a set membership approach, *Proc. Int. Symp. on Intelligent Robotic Systems*, Toulouse.

Drumheller, M.: 1987, Mobile robot localization using sonar, *IEEE Trans. on Pattern Analysis and Machine Intelligence* **9**(2), 325–332.

Elfes, A.: 1987, Sonar-based real-world mapping and navigation, *IEEE Journal of Robotics and Automation* **3**(3), 249–265.

Elfes, A.: 1991, Occupancy grids: A stochastic spatial representation for active robot perception, *in* S. S. Iyengar and A. Elfes (eds), *Autonomous Mobile Robots Perception, Mapping, and Navigation*, pp. 60–70.

Fox, D., Burgard, W. and Thrun, S.: 1998, Active Markov localization for mobile robots, *Robotics and Autonomous Systems* **25**(3-4), 195–207.

Fox, D., Burgard, W. and Thrun, S.: 1999, Markov localization for mobile robots in dynamic environments, *Journal of Artificial Intelligence Research* **11**, 391–427.

Garulli, A. and Vicino, A.: 2001, Set membership localization of mobile robots via angle measurements, *IEEE Transactions on Robotics and Automation* **17**(4), 450–463.

Gibbens, P. W., Dissanayake, G. M. W. M. and Durrant-Whyte, H. F.: 2000, A closed form solution to the single degree od freedom simultaneous localisation and map building (slam) problem, *Proc. IEEE Int. Conf. Decision and Control*, Sydney, Australia.

Hanebeck, U. D. and Horn, J.: 1999, A new estimator for mixed stochastic and set theoretic uncertainty models applied to mobile robot localization, *Proc. IEEE Int. Conf. Robotics and Automation*, Vol. 2, pp. 1335–1340.

Hanebeck, U. D. and Schmidt, G.: 1996, Set theoretical localization of fast mobile robots using an angle measurement technique, *Proc. IEEE Int. Conf. Robotics and Automation*, pp. 1387–1394.

Holenstein, A. A. and Badreddin, E.: 1992, Mobile-robot position update using ultrasonic range measurements, *International Journal of Robotics and Automation* **9**(2), 72–80.

Jensfelt, P. and Kristensen, S.: 1999, Active global localisation for a mobile robot using multiple hypothesis tracking, *Proc. of the IJCAI-99 Workshop on Reasoning with Uncertainty in Robot Navigation*, Stockholm, Sweden.

Kieffler, M., Jaulin, L., Walter, E. and Meizel, D.: 1999, Nonlinear identification based on unreliable priors and data, with application to robot localization, *in* A. Garulli, A. Tesi and A. Vicino (eds), *Robustness in Identification and Control*, Springer-Verlag, London.

Korte, B. and Vygen, J.: 2000, *Combinatorial Optimization: Theory and Algorithms*, Springer, New York.

Kurz, A.: 1996, Constructing maps for mobile robot navigation based on ultrasonic range data, *IEEE Trans. on System Man Cybernetics - Part B: Cybernetics* **26**(2), 233–242.

Kurzhanski, A. B. and Veliov, V. M.: 1994, *Modeling Techniques for Uncertainty Systems*, Birkhäuser, Boston.

Lacroix, S., Mallet, A., Chatila, R. and Gallo, L.: 1999, Rover self localization in planetary-like environments, *5th International Symposium on Artificial Intelligence, Robotics and Automation in Space*.

Leonard, J. J. and Durrant-Whyte, H. F.: 1991, Mobile robot localization by tracking geometric beacons, *IEEE Transactions on Robotics and Automation* **7**(3), 376–382.

Leonard, J. J. and Durrant-Whyte, H. F.: 1992, *Directed Sonar Sensing for Mobile Robot Navigation*, Kluwer Academic Publisher, Boston.

Levitt, T. S. and Lawton, D. T.: 1990, Qualitative navigation for mobile robots, *Artificial Intelligence* **44**(3), 305–360.

Mataric, M. J.: 1992, Environment learning using a distributed representation, *IEEE Transactions on Robotics and Automation* **8**(3), 304–312.

Milanese, M., Norton, J. P., Piet-Lahanier, H. and Walter, E. (eds): 1996, *Bounding Approaches to System Identification*, Plenum Press, New York.

Milanese, M. and Vicino, A.: 1991, Optimal estimation theory for dynamic systems with set membership uncertainty: an overview, *Automatica* **27**(6), 997–1009.

Mouaddib, E. M. and Marhic, B.: 2000, Geometrical matching for mobile robot localization, *IEEE Transactions on Robotics and Automation* **16**(5), 542–552.

Moutarlier, P. and Chatila, R.: 1989, Stochastic multisensory data fusion for mobile robot location and environment modelling, *Proceedings of the 5th International Symposium of Robotic Research*, pp. 207–216.

Olson, C. F.: 2000, Probabilistic self-localization for mobile robots, *IEEE Transactions on Robotics and Automation* **16**(1), 55–66.

Pshenichnyi, B. N. and Pokotilo, V. G.: 1983, A minimax approach to the estimation of linear regression parameters, *Eng. Cybernetics* pp. 77–85.

Reuter, J.: 2000, Mobile robot self-localization using PDAB, *Proc. IEEE Int. Conf. on Robotics and Automation ICRA'00*, San Francisco, CA.

Roumeliotis, S. and Bekey, G.: 2000, Bayesian estimation and Kalman filtering: a unified framework for mobile robot localization, *Proc. IEEE Int. Conf. on Robotics and Automation ICRA'00*, San Francisco, CA.

Sabater, A. and Thomas, F.: 1991, Set membership approach to the propagation of uncertain geometric information, *Proc. IEEE Int. Conf. Robotics and Automation*, Vol. 3, Sacramento, CA, pp. 2718–2723.

Shastri, S. (ed.): 1999, *Special Issue on Field and Service Robotics*, number 18:7 in *International Journal of Robotics Research*, Sage Publications.

Sutherland, K. T. and Thompson, W. B.: 1994, Localizing in unstructured environments: dealing with the errors, *IEEE Transactions on Robotics and Automation* **10**(6), 740–754.

Talluri, R. and Aggarwal, J. K.: 1992, Position estimation for an autonomous mobile robot in an outdoor environment, *IEEE Transactions on Robotics and Automation* **8**(5), 573–584.

Thrun, S., Burgard, W. and Fox, D.: 1998, A probabilistic approach to concurrent mapping and localization for mobile robots, *Machine Learning,* 31:29-53 and *Autonomous Robots,* 5:253-271 . Joint issue.

Uhlmann, J. K., Julier, S. J. and Csorba, M.: 1997, Nondivergent simultaneous map building and localization using covariance intersection, *SPIE-Int. Soc. Opt. Eng. Proceedings of Spie - the International Society for Optical Engeneering*, Orlando, FL, pp. 2–11.

Vicino, A. and Zappa, G.: 1996, Sequential approximation of feasible parameter sets for identification with set membership uncertainty, *IEEE Transactions on Automatic Control* **41**, 774–785.

Victorino, A. C., Rives, P. and Borrelly, J.-J.: 2002, A realtive motion estimation using a bounded error method, *Proc. IEEE/RSJ Int. Conf. Intelligent Robots and Systems*, Vol. 1, Lausanne, CH, pp. 643–648.